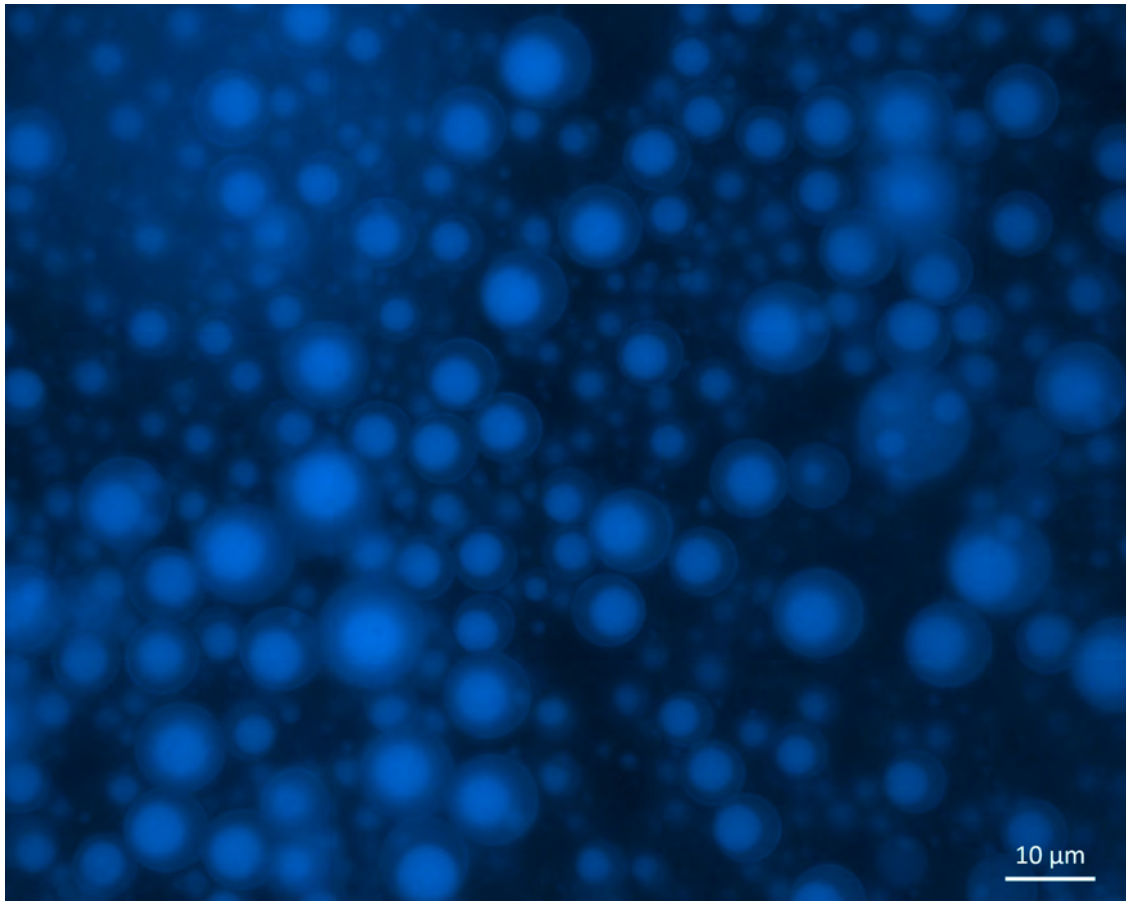




**CHALMERS**  
UNIVERSITY OF TECHNOLOGY

---



# **Microencapsulation of cationic antimicrobial surfactants in core-shell particles**

---

Master's thesis in Materials Chemistry

EMIL LUKASIEWICZ

---

Department of Chemistry and Chemical Engineering  
CHALMERS UNIVERSITY OF TECHNOLOGY  
Gothenburg, Sweden 2019



MASTER'S THESIS 2019

# Microencapsulation of cationic antimicrobial surfactants in core-shell particles

EMIL LUKASIEWICZ



**CHALMERS**  
UNIVERSITY OF TECHNOLOGY

Department of Chemistry and Chemical Engineering  
*Division of Applied Chemistry*  
CHALMERS UNIVERSITY OF TECHNOLOGY  
Gothenburg, Sweden 2019

Microencapsulation of cationic antimicrobial surfactants in core-shell particles

EMIL LUKASIEWICZ

© EMIL LUKASIEWICZ, 2019.

Supervisor: Lars Nordstierna, Department of Chemistry and Chemical Engineering

Supervisor: Markus Andersson Trojer, RISE IVF

Examiner: Lars Nordstierna, Department of Chemistry and Chemical Engineering

Master's Thesis 2019

Department of Chemistry and Chemical Engineering

Division of Applied Chemistry

Chalmers University of Technology

SE-412 96 Gothenburg

Cover: Picture taken with fluorescence microscope (100x magnification) visualizing core-shell particles of PLGA consisting of ethyl linoleate, benzalkonium chloride and pyrene.

Gothenburg, Sweden 2019

EMIL LUKASIEWICZ

Department of Chemistry and Chemical Engineering

Chalmers University of Technology

## Abstract

Within the health care industry, there has been an increasing frequency of non-healing chronic wounds. This development is associated with an increasing portion of the population being older. Momentarily, the issue is addressed with various antiseptics that are impregnated in wound care dressings. The concentration of antiseptics is a vital design parameter. If the antibacterial substance is impregnated in the wound care dressing material, an excess of antibacterial substance is needed to retain a concentration above the minimum inhibitory concentration and multiresistant development will become a significant risk. To control the release for a prolonged time and decrease the risk of multiresistant development, microencapsulation is suggested.

In this project, a formulation pathway of microcapsules consisting of a biocompatible polymer encapsulating a cationic antibacterial substance dissolved in a biocompatible core oil has been investigated. The focus has been on formulating microcapsules with a core-shell morphology. The solubility of the two active substances benzalkonium chloride and octenidine dihydrochloride in a number of biocompatible oils has been investigated, which is prerequisite along with satisfactory spreading coefficients between the oil, polymer and the continuous aqueous phase. Eventually, the solubility tests led to two distinct pathways of the project; 1) microencapsulation attempts of benzalkonium chloride with modified internal phase separation by solvent evaporation and 2) modification of octenidine dihydrochloride to improve solubility in the core oils of interest. Microencapsulation of benzalkonium chloride led to enabled core-shell morphology for a range of various oils, with the possible exception of jojoba oil and glyceryl tributanoate. Although non-central cores could be observed, NMR spectroscopy indicated that benzalkonium chloride was encapsulated, in spite of being water-soluble. The modified, deprotonated octenidine conveyed no improved solubility. Microsphere formulation and interfacial tension measurements of both octenidine dihydrochloride and the modified compound suggested similar properties in terms of surface activity.

Keywords: microencapsulation, core-shell, acorn, interfacial spreading, solubility, microscopy, PLGA, ethyl linoleate, benzalkonium chloride, octenidine dihydrochloride.



## Acknowledgements

Firstly, I want to thank Lars Nordstierna for the opportunity to work with you and the supervision and guidance. It has been a truly rewarding experience.

I want to thank Markus Andersson Trojer, whose expertise in the field of microencapsulation formulation and overall commitment has provided knowledge and inspiration during the course of the project.

I want to thank Anna-Karin Hellström, Mats Hulander and Romain Bordes at the Division of Applied Chemistry, who have provided valuable inputs, guidance and inspiration throughout the project, ranging from utilization of the microscope and the modification of active substances.

Lastly, a special thanks to Viktor Eriksson, Petrus Jakobsen, Alice Flodin and all the students in the master thesis room at Applied Chemistry, for interesting and valuable talks and conversations of both project-related and non-project-related subjects.

Emil Lukasiewicz, Gothenburg, June 2019





# Contents

<b>List of Figures</b>	<b>xiii</b>
<b>List of Tables</b>	<b>xv</b>
<b>1 Introduction</b>	<b>1</b>
1.1 Background . . . . .	1
1.2 Aim . . . . .	2
1.3 Limitations . . . . .	2
1.4 Specification of issue under investigation . . . . .	2
<b>2 Theory</b>	<b>3</b>
2.1 Microcapsules and microencapsulation . . . . .	3
2.1.1 Fluorophores . . . . .	5
2.1.2 Interfacial spreading . . . . .	5
2.2 Internal phase separation by solvent evaporation . . . . .	6
2.3 Polymers . . . . .	7
2.3.1 Poly(lactic-co-glycolic acid)(PLGA) . . . . .	7
2.4 Core oils . . . . .	8
2.4.1 Ethyl linoleate . . . . .	8
2.4.2 Docosahexanoic acid methyl ester (DHA) . . . . .	8
2.4.3 Jojoba oil . . . . .	9
2.4.4 Glyceryl tributanoate . . . . .	9
2.4.5 Glyceryl trioctanoate . . . . .	10
2.4.6 Olive oil . . . . .	10
2.4.7 Sunflower oil . . . . .	10
2.5 Active substances . . . . .	11
2.5.1 Benzalkonium chloride . . . . .	11
2.5.2 Octenidine dihydrochloride . . . . .	11
2.6 Dispersants . . . . .	12
2.6.1 Polyvinyl alcohol (PVA) . . . . .	12
2.7 Analytical techniques . . . . .	13
2.7.1 Bright field (light) & fluorescence microscopy . . . . .	13
2.7.2 Interfacial tension & pendant drop method . . . . .	15
2.7.2.1 Gibbs adsorption isotherm . . . . .	15
2.7.3 Nuclear Magnetic Resonance Spectroscopy (NMR) . . . . .	15

<b>3</b>	<b>Methods</b>	<b>17</b>
3.1	Chemicals and Materials . . . . .	17
3.2	Solubility of active substances in core oils . . . . .	18
3.3	Internal phase separation by solvent evaporation . . . . .	18
3.3.1	Microcapsule formulation . . . . .	18
3.3.2	Characterization of microcapsules . . . . .	19
3.4	Deprotonated octenidine . . . . .	19
3.4.1	Deprotonation of octenidine dihydrochloride. . . . .	20
3.4.2	Microsphere formulation of deprotonated octenidine . . . . .	21
3.4.3	Interfacial tension measurements of octenidine dihydrochloride and deprotonated octenidine . . . . .	21
<b>4</b>	<b>Results &amp; Discussion</b>	<b>23</b>
4.1	Solubility of cationic antimicrobial surfactans in biocompatible oils . .	23
4.1.1	Solubility & influence of heat . . . . .	24
4.2	Microcapsule formulation: Benzalkonium chloride . . . . .	25
4.2.1	Core-shell systems . . . . .	25
4.2.2	Size distributions of core-shell microcapsules . . . . .	27
4.2.3	Jojoba oil . . . . .	28
4.2.4	Partition of benzalkonium chloride between microcapsules and aqueous phase . . . . .	30
4.3	Deprotonation of octenidine dihydrochloride . . . . .	32
4.3.1	Microsphere formulation of deprotonated octenidine . . . . .	34
4.3.2	Interfacial tension measurements of octenidine dihydrochloride and deprotonated octenidine . . . . .	35
<b>5</b>	<b>Conclusion</b>	<b>37</b>
<b>A</b>	<b>Microscopy images from the benzalkonium chloride encapsulation</b>	<b>I</b>
<b>B</b>	<b>Yield of deprotonated octenidine</b>	<b>V</b>
<b>C</b>	<b>Interfacial tension measurements for deprotonated octenidine and octenidine dihydrochloride</b>	<b>VII</b>

# List of Figures

2.1	The morphologies of microcapsules. Microcapsules could be homogeneous (a), single (b) or multi-core (c), possess several cavities (d) or acorn (e). . . . .	4
2.2	The molecular structure of a fluorophore, pyrene. . . . .	5
2.3	A schematic illustration of the formation of microcapsules when internal phase separation by solvent evaporation is employed. . . . .	7
2.4	The molecular structure of Poly(lactic-co-glycolic acid)(PLGA). . . . .	8
2.5	The molecular structure of ethyl linoleate. . . . .	8
2.6	The molecular structure of docosahexanoic acid methyl ester (DHA). . . . .	9
2.7	11-Eicosenoic acid, the predominant compound in jojoba oil. . . . .	9
2.8	The molecular structure of glyceryl tributanoate. . . . .	10
2.9	The molecular structure of glyceryl trioctanoate. . . . .	10
2.10	The molecular structure of benzalkonium chloride when the aliphatic chain constitute of 12 carbons (n=12). . . . .	11
2.11	The molecular structure of octenidine dihydrochloride. The notions of (2) and (3) will referenced in section 4.3. . . . .	12
2.12	The molecular structure of polyvinyl alcohol (PVA). . . . .	13
2.13	Schematic illustration of bright field microscopy. (Modified) [51] . . . . .	14
2.14	The setup of fluorescence microscopy. [52] . . . . .	14
3.1	The molecular structure of deprotonated octenidine. The notion of (3) will referenced in section 4.3. . . . .	20
4.1	Microcapsules with ethyl linoleate observed with fluorescence microscopy (100x magnification). . . . .	26
4.2	Microcapsules with docosahexanoic acid methyl ester observed with fluorescence microscopy (100x magnification). . . . .	27
4.3	Size distributions of all core-shell systems involving benzalkonium chloride with a lognormal fitting. . . . .	28
4.4	Microcapsules with jojoba oil observed with bright field microscopy (100x magnification), where (b) and (c) highlights the appearance of acorn. . . . .	29

---

4.5	NMR spectra for reference sample with benzalkonium chloride and heavy water (upper image) and benzalkonium chloride encapsulated with ethyl linoleate in PLGA microcapsules (lower image). Milli-Q-water was exchanged with heavy water in the aqueous phase. The chemical shift (ppm) at the x-axes. The signal at (1) correspond to the aromatic ring in benzalkonium chloride, see Figure 2.10. . . . .	31
4.6	Superimposed NMR spectra in the 7.23-7.42 ppm range for reference sample with benzalkonium chloride and heavy water (upper image) and benzalkonium chloride encapsulated with ethyl linoleate in PLGA microcapsules with heavy water as aqueous phase (lower image). The chemical shift (ppm) at the x-axes. . . . .	32
4.7	The state of the filtered water after vacuum filtration. . . . .	33
4.8	NMR spectra for octenidine dihydrochloride (upper image) and deprotonated octenidine dihydrochloride (lower image). The chemical shift (ppm) at the x-axis. The signals at (2) and (3) correspond to significant signals for octenidine dihydrochloride and deprotonated octenidine. Corresponding protons are illustrated in Figure 2.11 for octenidine dihydroachloride and Figure 3.1 for deprotonated octenidine. . . . .	34
4.9	Microspheres with deprotonated octenidine observed in microscopy, with 0 wt% of deprotonated octenidine at the left, 5 % deprotonated octenidine represented in the middle and 10 wt% deprotonated octenidine at the right. 100x magnification for all images. . . . .	35
4.10	The interfacial tensions of octenidine dihydrochloride and deprotonated octenidine as a function of logarithmic bulk concentration. . . . .	36
A.1	A representative image of ethyl linoleate/benzylkonium chloride microcapsules, obtained from bright field microscopy (100x magnification). . . . .	I
A.2	Two representative images of olive oil/benzalkonium chloride microcapsules, obtained from (a) bright field and (b) fluorescence microscopy (both 100x magnification). . . . .	II
A.5	A representative image of docosahexanoic acid methyl ester/benzylkonium chloride microcapsules, obtained from bright field microscopy (100x magnification). . . . .	II
A.3	Two representative images of glyceryl trioctanoate/benzalkonium chloride microcapsules, obtained from (a) bright field and (b) fluorescence microscopy (both 100x magnification). . . . .	III
A.6	A representative image of jojoba oil/benzylkonium chloride microcapsules, obtained from fluorescence microscopy (100x magnification). . . . .	III
A.4	Two representative images of sunflower oil/benzalkonium chloride microcapsules, obtained from (a) bright field (40x magnification) and (b) fluorescence microscopy (100x magnification). . . . .	IV

# List of Tables

3.1	The recipe for the microcapsule formulations. . . . .	19
3.2	The microsphere formulations involving encapsulation of deprotonated octenidine. . . . .	21
3.3	The samples for interfacial tension measurements. The stock solution contained 0.0025 g of active substance and 10 g of dichloromethane (0.33 mg/ml). . . . .	22
4.1	Solubility of benzalkonium chloride in biocompatible oils. . . . .	23
4.2	The solubility tests involving heat treatment. The star (*) indicate systems which became opaque after the tests and actual confirmation of solubility. . . . .	24
4.3	Observed morphology for systems involving 1wt% benzalkonium chloride. . . . .	25
4.4	The Gibbs adsorption isotherm for deprotonated octenidine and octenidine dihydrochloride. The parenthesis is the isotherm for deprotonated octenidine if the compound is assumed to be uncharged (n=1). . . . .	36
C.1	Interfacial tension of deprotonated octenidine (DPO) and octenidine dihydrochloride (OCT) as a function of weight percent. The compounds were dissolved in dichloromethane and immersed in 5 wt% PVA-water-solution. . . . .	VII



# 1

## Introduction

In the following sections, the background, aim and limitations of the project will be outlined. Furthermore, the purpose of this project will be specified.

### 1.1 Background

Within the health care industry, the issue of an increasing frequency of non-healing chronic wounds has in the recent decades become more palpable. Non-healing chronic wounds are heavily associated with an ageing population, and the consequences range from deterioration in quality of life to mortality. The economic costs accompanied with non-healing chronic wounds have increased over the years as the population have become older.[1] In Sweden by the year 2030, the population that are 65 years old or older will constitute a quarter of the total population.[2]

Another growing health issue associated with non-healing wounds and an ageing population is the increasing prevalence of diabetes (*Diabetes mellitus*). The number of people affected by diabetes is projected to increase in the future.[3] Consequently, the prevalence of Diabetic foot ulcers (DFU) will become more frequent. Diabetic foot ulcers appear due to reduced blood flow for diabetic patients which hinders cell growth in the affected area (predominantly lower extremities).[4]

At the moment, these issues are addressed by the use of various antiseptics that are impregnated into wound care dressings. An important design parameter regarding wound care dressings is the concentration of the antiseptics in the wound. The critical concentration of antiseptics in which multiresistant development will not occur is referred as the minimum inhibitory concentration (MIC).

A simple impregnation leads to active and uncontrolled release of the antibacterial substance, thus having a concentration of the antibacterial substance below MIC within a relatively short period of time. Consequently, the tendency for multiresistant development will become more significant.[5] A suggested solution to this issue is to encapsulate the antibacterial substance in so called microcapsules. By encapsulating the antibacterial substance, a controlled release is enabled, where the concentration of antiseptics could be maintained above the minimum inhibitory concentration (MIC) for a prolonged period of time, thus hindering the development of multiresistant bacteria.

A group of substances that are of interest due to the inhibiting effect on multiresistant development and low cytotoxicity are cationic antimicrobial surfactants, often referred to as QAC (Quaternary Ammonium Compounds).[6] Examples of cationic antimicrobial surfactants are benzylkonium chloride and octenidine dihydrochloride.

### **1.2 Aim**

The aim of this project is to find a formulation pathway of microcapsules consisting of a biocompatible polymer shell, biocompatible core oil and a cationic antimicrobial substances (QAC) encapsulated. Primarily, this involves 1) investigation of solubility of cationic antimicrobial substances in biocompatible oils (see section 3.2) and 2) finding components which satisfy the spreading conditions, see section 2.1.2. The spreading coefficients will dictate whether the different capsule components will dissociate or form distinct phases which will constitute a core-shell morphology. The formulation method of interest is internal phase separation by solvent evaporation.

### **1.3 Limitations**

The project is limited to the formulation of microcapsules, with a focus on core-shell particles. The shell materials of interest are biobased polymers, since the application of interest is within the field of health care. The core will consist of a biocompatible oil and a cationic antibacterial substance. The oils is restricted to biological fatty acids, whereas the antibacterial substances are limited to cationic antimicrobial surfactants. Specifically, the antibacterial substance are limited to benzalkonium chloride and octenidine dihydrochloride. Moreover, the formulation of microcapsules will be employed through internal phase separation by solvent evaporation. No other method of formulation will be taken into account in this project.

### **1.4 Specification of issue under investigation**

The project will investigate the possibilities of formulating core-shell particles in which a biocompatible polymer shell is encapsulating an oil phase consisting of a biocompatible oil and a cationic antimicrobial surfactant.

# 2

## Theory

In the following section, the theoretical foundation will be outlined. Initially, the concept of microcapsules and how the morphology of microcapsules are dictated by the interfacial tension properties of the three phases (polymer, core oil, continuous aqueous phase) will be treated. Furthermore, the concept of the formulation method of interest (internal phase separation by solvent evaporation) will be explained. Subsequently, compounds of interest for the different phases (polymer, core oil, active substance and dispersant) are further detailed. Lastly, the theoretical background for the techniques and methods to analyze the results will be addressed.

### 2.1 Microcapsules and microencapsulation

For the purpose of encapsulating an active substance, colloidal systems have become increasingly interesting from a scientifically point of view. The use of colloidal systems for encapsulating active substances have enabled improvements in several application areas. In food technology, masking unpleasant flavors in food products and increasing shelf life of an active substance are examples of improvements when utilizing colloidal systems for encapsulation. Other areas of use includes agriculture, cosmetics and detergency. However, the drawback of using traditional colloidal systems for encapsulation of an active substances are the difficulties to control the release profile. For the purpose of controlling the release of an active substance, microcapsules are considered to possess a greater potential than traditional colloidal systems.[7]

Microencapsulation is the concept of coating solid particles, liquid droplets or gas bubbles (which constitute the core) with a film of a so called shell material. The size of microcapsules are normally within the range of 0.1-1000  $\mu\text{m}$ . Microencapsulation is utilized in a wide range of applications depending on aim and purpose. In general, microcapsules are used to protect certain substances and/or govern the release of them.[8] In the pharmaceutical field, transportation reservoirs of drugs is a common application of microcapsules. The use of microcapsules in the pharmaceutical industry provides several advantages; it enables substantially extensive control over the drug release and it effectively protects the active agent from enzymatic degradation in the body.[9] In formulation of coatings and paints, it is important that coatings and paints are able to protect themselves from biofouling. In order to achieve protection from biofouling, biocides are incorporated.[8] Biocides are defined according to EU (Regulation (EU) No. 528/2012, BPR) as chemical substances or microor-

organisms which purpose is to deter or control the prevalence of harmful organisms by chemical or biological means [10]. One of the main issues when incorporating biocides in paint/coatings is the fast diffusion out from a coated surface to the surroundings. In order to control the surface flux of biocides and enable longevity in the protection from biofouling, the biocides can be encapsulated in microcapsules. Encapsulation allows lower amount of biocides utilized, in comparison if the biocides would be freely disperse in the coating/paint matrix.[8]

Microcapsules can be formulated in a wide range of different shapes, sizes and morphologies. With regards to morphology, there are four major classes. In the microspheres, the active substance is incorporated within the polymer matrix (see Figure 2.1a). Single-shell and multi-shell constitute another class, where a hollow center is surrounded by either one shell or several shells (see Figure 2.1b and 2.1c). A third class is poly-core, where several cavities are incorporated within the shell (Figure 2.1d).[11] If phase separation would occur, the two phases would either be separated completely (droplet separation) or form an acorn morphology (see Figure 2.1e).[8] To achieve a certain morphology, one has to take into account the materials of choice and selected microencapsulation method. Primarily, by knowing the interfacial properties of the materials, prediction of morphology is enabled as described in the subsequent section.[11]

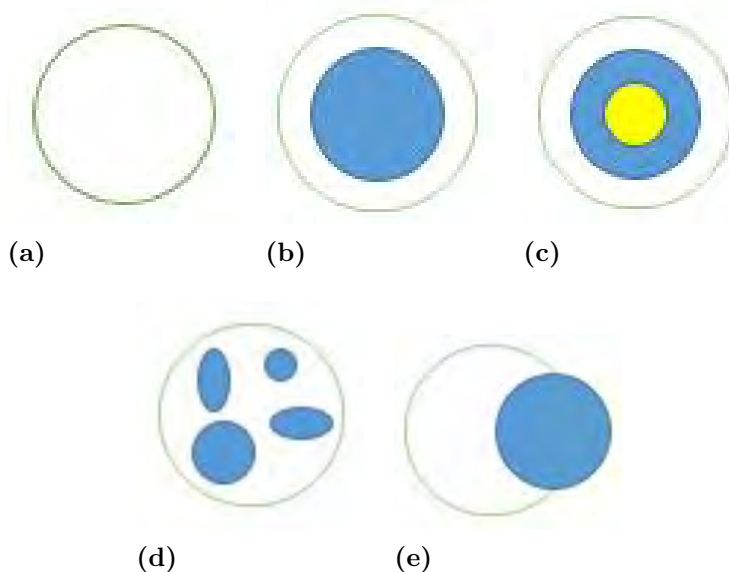


**Figure 2.1:** The morphologies of microcapsules. Microcapsules could be homogeneous (a), single (b) or multi-core (c), possess several cavities (d) or acorn (e).

In comparison with the aforementioned morphologies, core-shell particles provides several benefits. Improved stability, wear-resistance [12] and an additional amount of degrees of freedom with regards to controlling the release profile of an active substances (in comparison with microspheres) are some of the benefits provided by core-shell morphology.[7]

### 2.1.1 Fluorophores

A common aid for visualization of microcapsule morphology are fluorophores. Fluorophores are molecules that exhibit measureable fluorescence when excited [13]. One example of a commonly used fluorophore is pyrene. The photophysical properties of pyrene (Figure 2.2) are well-known. Pyrene absorb UV-light at several distinct wavelengths between 200 and 400 nm [14]. Due to its distinctive fluorescence bands and high fluorescence quantum yield, it is employed as molecular probe for microenvironments. For instance, these particular fluorescence properties have been exploited in the research of water-soluble polymers during the last 50 years. Another area of application is characterization of surfactant micellar systems.[15] Besides the photophysical benefits, pyrene could provide catalytic benefits due to its  $\pi$ -stacking abilities [14]. Pyrene is soluble in organic solvents such as ethanol, ethyl ether and benzene.[16]

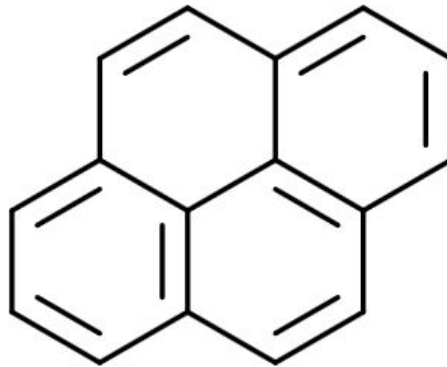


**Figure 2.2:** The molecular structure of a fluorophore, pyrene.

### 2.1.2 Interfacial spreading

The morphology of microcapsules in a three-phase system is dependent on the wetting ability for each phase, namely the polymer, oil and aqueous phase. The wetting abilities are described by the interfacial tension between each phase. The overall contribution of each interface is described by the spreading coefficients. For a three phase system consisting of a polymer, oil and aqueous phase, the spreading coefficient for the polymer is illustrated in equation 2.1.

$$S_P = \gamma_{OW} - (\gamma_{PO} + \gamma_{PW}) \quad (2.1)$$

Where the subscript of P, O and W stands for the polymer, oil and aqueous phase, respectively. Depending on how the interfacial tension forces are balancing and subsequently, which signs of the spreading coefficients are obtained, the morphology can be assigned for a particular system. In terms of spreading coefficients, following conditions have to be fulfilled for core-shell morphology (equation 2.2):

$$\begin{cases} S_P > 0 \\ S_O < 0 \\ S_W < 0 \end{cases} \quad (2.2)$$

It should be noted that a precondition for enabling  $S_P > 0$ , the interfacial tension between oil and water has to be greater than the interfacial tension between polymer and oil ( $\gamma_{OW} > \gamma_{PO}$ ).[8]

Acorn morphology appears when there is marginal wetting between the phases [17]. In terms of spreading coefficients, all of them (equation 2.2) are negative in that case. A complete oil and polymer separation is obtained when the spreading coefficient of the oil is negative, whereas the spreading coefficients of the polymer and aqueous phase are positive. Regarding microspheres, it should be noted that this description is not applicable since the polymer and the water phase are the only phases present.[8]

## 2.2 Internal phase separation by solvent evaporation

Internal phase separation by solvent evaporation is a formulation method of microcapsules developed by Loxley and Vincent [18]. An oil-in-water-emulsion is formulated by dissolving a polymer, core oil and an active substance in a volatile solvent. This solution will be the dispersive oil phase. In the formulation prepared by Loxley and Vincent, dichloromethane was used as the volatile solvent along with a minor fraction of acetone to improve the emulsification process. Dichloromethane has the beneficiary properties as volatile solvent and low miscibility in water. The continuous aqueous phase contains Milli-Q-water and a dispersant. The benefits of internal phase separation by solvent evaporation is that relatively thick shells can be achieved, narrow size distributions can be enabled and it is suitable for the purpose of encapsulating an oil. Furthermore, by tuning the oil/polymer-ratio, the method provides control and predictability of the release profile of an encapsulated active substance. The drawbacks of utilizing this method is that an organic solvent is required.[17] An illustration of microcapsule formation by the method developed by Loxley and Vincent is visualized in Figure 2.3.

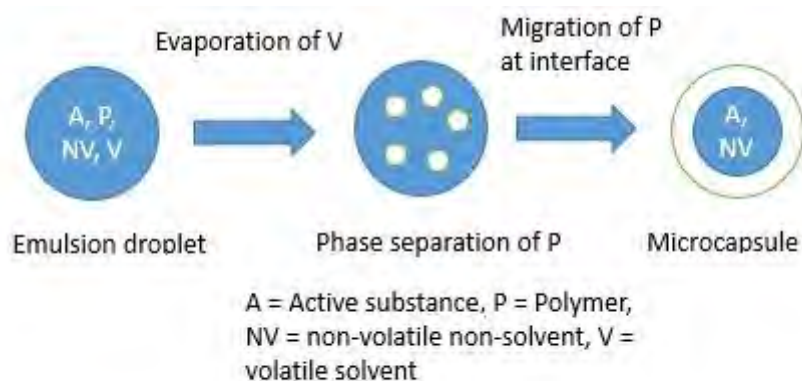


**Figure 2.3:** A schematic illustration of the formation of microcapsules when internal phase separation by solvent evaporation is employed.

## 2.3 Polymers

There are numerous requirements that has to be fulfilled in order for a polymer to be a candidate for investigation in this project. The polymer has to be biodegradable, biocompatible and possess low toxicity, due to the intended health care application.[19] There has been extensive research regarding natural biodegradable polymers for the purpose of drug delivery. Nevertheless, natural biodegradable polymers are associated with high cost and low purity. Instead, synthetic biodegradable polymers have become more interesting for the purpose of extended drug release [20].

### 2.3.1 Poly(lactic-co-glycolic acid)(PLGA)

One example of a synthetic, biodegradable polymers that is extensively used in microencapsulation of antigens and therapeutics is poly(lactic-co-glycolic acid) (PLGA) [21]. A specific encapsulation purpose involving PLGA is the encapsulation of active substances for nasal drug delivery [22]. Poly(lactic-co-glycolic acid) is a copolymer of lactic acid units and glycolic acid units, see Figure 2.4. Since the glycolic acid unit is more hydrophilic than the lactic acid unit, the ratio between lactic acid units and glycolic acid units will govern its physiochemical properties. For instance, lactide-rich PLGA will degrade at a lower rate and absorb less water than glycolic-rich PLGA.[19] Furthermore, PLGA with a ratio of 50:50 have a higher tendency to undergo hydrolysis than PLGA with unequal ratio of lactide acid units and glycolide acid units.[20, 22]

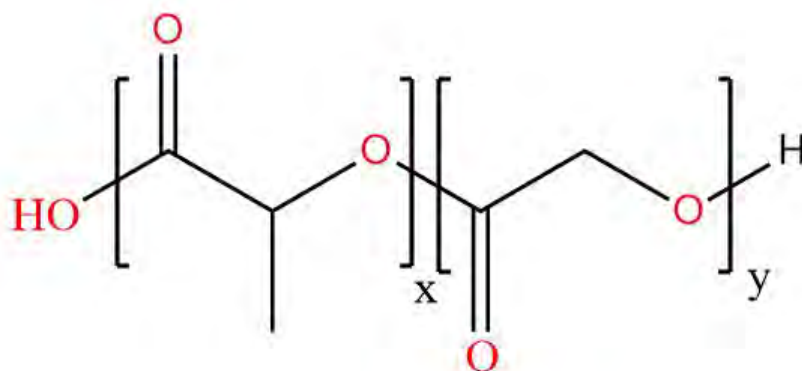


**Figure 2.4:** The molecular structure of Poly(lactic-co-glycolic acid)(PLGA).

## 2.4 Core oils

The purpose of using a core oil along with the active substance in the microcapsules is to control the diffusion of the active substance [23]. Since the microencapsulation is performed in the context of a health care, the core oil has to be biocompatible and have a low cytotoxicity. Alkanes have been treated in previous studies [18], but are not suitable for the intended application of health care [23]. A class of chemical compounds that fulfill the requirements and have been extensively studied in the context of microencapsulation are vegetable oils [24]. Other classes of compounds that fulfill the requirements and have proven health benefits are fatty acid esters [25] and triglycerides (see subsection 2.4.4 and 2.4.5). In following section, the oils of interest in this project will be introduced.

### 2.4.1 Ethyl linoleate

Ethyl linoleate (Figure 2.5) is a long-chain fatty acid ethyl ester, derived from linoleic acid. Due to its antibacterial and its anti-inflammatory properties, ethyl linoleate is a common constituent in cosmetics and pharmaceutical products.[26]

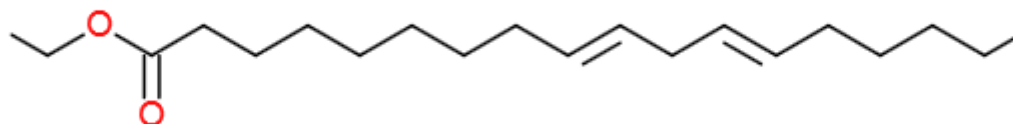


**Figure 2.5:** The molecular structure of ethyl linoleate.

### 2.4.2 Docosahexanoic acid methyl ester (DHA)

Docosahexanoic acid (DHA) is an  $\omega$ -3 polyunsaturated fatty acid which comprises of 22 carbons and 6 double bonds, see Figure 2.6 [27]. It is a component in cod liver

oil [28] and intake of DHA has been shown to be vital for health. An insufficient intake of DHA could lead to depression, cognitive deterioration when aging, cancer and heart diseases.[29]

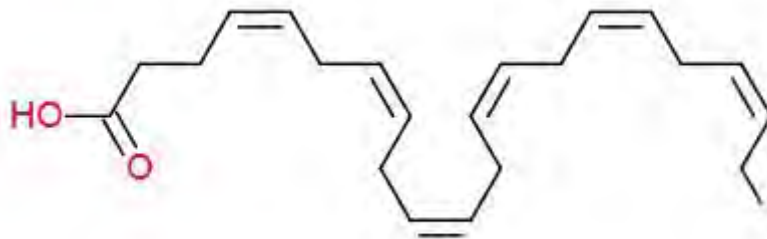


**Figure 2.6:** The molecular structure of docosahexanoic acid methyl ester (DHA).

### 2.4.3 Jojoba oil

Jojoba oil is a mixture of straight chained fatty acids and alcohols (predominantly  $C_{20}$  and  $C_{22}$ ) [30]. Eicosenoic and docosenoic acid are the primary fatty acids present in jojoba oil, along with their alcohol derivatives eicosanol and docosanol. The unsaturated 11-Eicosenoic acid (Figure 2.7) is the single most prevalent component in jojoba oil.[31] The oil is derived from the jojoba seeds of the *Simmondsia chinensis* plant, a plant mostly found in northwestern Mexico and southern Arizona. Due to its non-toxicity and biodegradability, jojoba oil is extensively utilized in cosmetics and hair care products. Furthermore, the oil is utilized as an antifoaming agent in the production of antibiotics. Other physical properties of jojoba oil are high viscosity (in contrast to petroleum oils), high stability and low volatility. The freezing point of jojoba oil is in the range of 7.0-10.6  $C^{\circ}$ .[30]

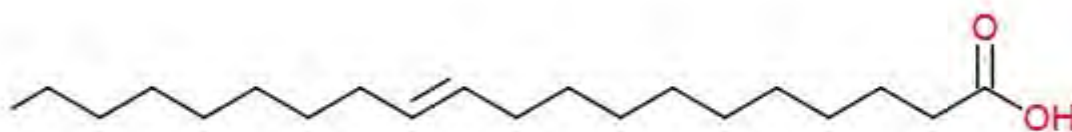


**Figure 2.7:** 11-Eicosenoic acid, the predominant compound in jojoba oil.

### 2.4.4 Glyceryl tributanoate

Glyceryl tributanoate is a saturated triglyceride, where glycerol is esterified with butyric acid (see Figure 2.8). Most notably, the compound is utilized as a food additive. Extensive research involving glyceryl tributanoate has been conducted within the field of pharmaceuticals.[32] Studies have shown the inhibitory effect on cancer cells and gram-negative bacteria that the compound possess [33, 34].

Furthermore, glyceryl tributanoate has shown to provide a positive effect on the cognitive abilities, i.e. retarding the development of Alzheimer's disease [32].

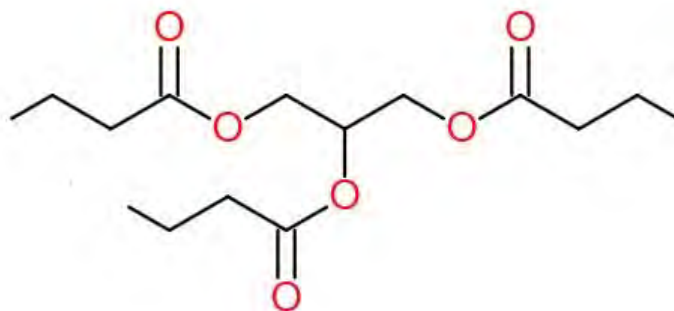


**Figure 2.8:** The molecular structure of glyceryl tributanoate.

### 2.4.5 Glyceryl trioctanoate

Glyceryl trioctanoate is a saturated triglyceride where glycerol has been esterified with three caprylic acid moieties (compare glyceryl tributanoate and butyric acid), see Figure 2.9. The compound is mainly used in cosmetics and in the pharmaceutical field, notably as a lubricant.[35]

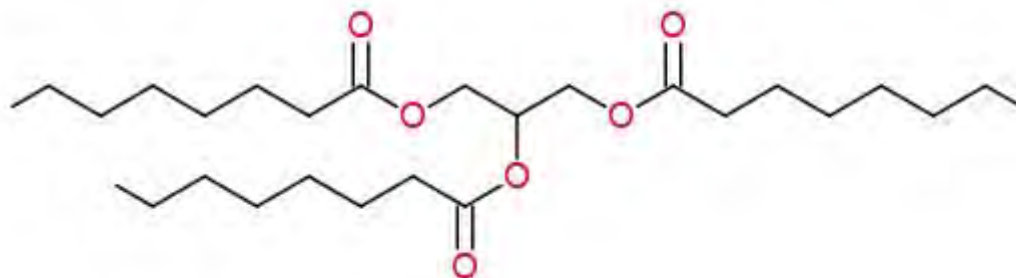


**Figure 2.9:** The molecular structure of glyceryl trioctanoate.

### 2.4.6 Olive oil

The main constituent in olive oil are triglycerides (~99%). In addition, free fatty acids and partial glycerides are prevalent in olive oil. Oleic acid is generally the most abundant fatty acid, where the content ranges from 55% to 83%. The second most abundant fatty acid is palmitic acid (7.5-20%). The composition depends on several factors, among those factors are the climate, zone of production and stage of maturity of the fruit.[36]

### 2.4.7 Sunflower oil

Sunflower oil constitute mainly of a mixture of triglycerides (~99%). The main fatty acids that are present are linoleic acid (18:2), oleic acid (18:1), palmitic acid (16:0)

and stearic acid (18:0). Commercially available sunflower oil is classified according to the relation between linoleic acid and oleic acid. There are three different classes, *regular* (high linoleic content), high-oleic and mid-oleic. In *regular* sunflower oil, the most abundant triglycerides are trilinolein (36.3%) and oleo-dilinolein (29.1%).[37]

## 2.5 Active substances

The purpose of the active substance is to pose an antibacterial effect on the chronic wound. The active substances of interest in this project are cationic antimicrobial substances. Specifically, the two cationic antimicrobial substances of interest are benzalkonium chloride and octenidine dihydrochloride.

### 2.5.1 Benzalkonium chloride

Benzalkonium chloride is an alkylbenzyl dimethylammonium compound where the aliphatic chain could be of various length. From a commercial perspective, the number of carbons which constitute the aliphatic chain varies among 12 (see Figure 2.10), 14 and 16.[38] Benzalkonium chloride is utilized in a wide range of applications. Within the chemical industry, benzalkonium chloride is mainly used as a surfactant in household and industrial products, a biocide due to its antimicrobial properties and as a phase transfer agent [39, 40]. Benzalkonium chloride has been reported to have a decreasing cytotoxic effect with increasing concentration, partially due to micelle formation being induced.[38]. The alkyl derivatives with a chain length of 12 and 14 have been reported to be water soluble, whereas the alkyl derivative with a chain length of 16 is poorly soluble.[41]

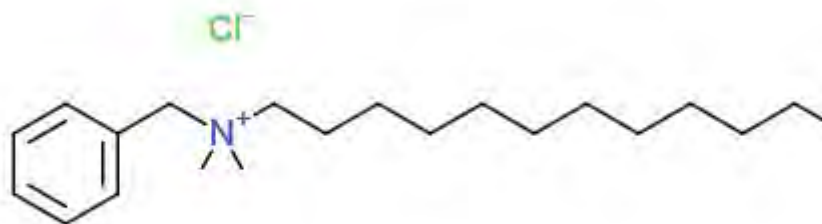


**Figure 2.10:** The molecular structure of benzalkonium chloride when the aliphatic chain constitute of 12 carbons ( $n=12$ ).

### 2.5.2 Octenidine dihydrochloride

Octenidine dihydrochloride is a gemini-type surfactant widely used as an antiseptic agent, primarily for the healing of wounds and mucosal infections [42]. It is effective against gram-negative bacteria, gram-positive bacteria and fungi. The compound comprises of two cationic groups separated by 10  $\text{CH}_2$ -groups. It is stable in a

broad pH range (1.6-12.2) and insensitive to light and hydrolysis.[43]. The  $pK_a$  of octenidine dihydrochloride is 10.89.[44]

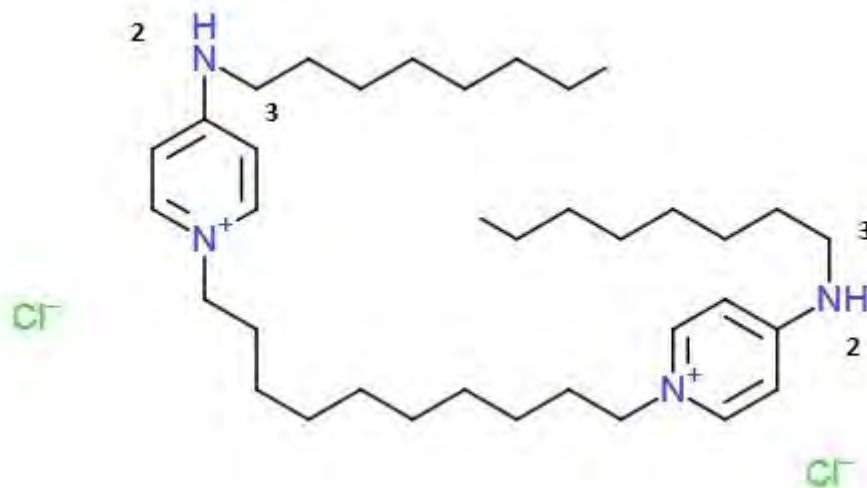


**Figure 2.11:** The molecular structure of octenidine dihydrochloride. The notions of (2) and (3) will be referenced in section 4.3.

## 2.6 Dispersants

The purpose of using a dispersant in the continuous phase is to stabilize the dispersion, ensuring that particle aggregation will not occur. There are two different possible mechanisms for dispersion stabilization, electrostatic and steric stabilization. With electrostatic stabilization, counterions are introduced which attract to the negatively charged particles. When particles approach each other, there will be regions of high counterion concentration, leading to water diffusing in these regions to separate them. The driving force is osmotic pressure. Steric stabilization is enabled by the same driving force as with electrostatic stabilization. Instead of introducing counterion, steric molecules (polymers) are attached to the particles.[45] In this project, polyvinyl alcohol (which sterically stabilizes) has been used as a dispersant.

### 2.6.1 Polyvinyl alcohol (PVA)

Polyvinyl alcohol (abbreviated to PVA) is a synthetic, water-soluble polymer which is synthesized from polyvinyl acetates by deacetylation of the acetates group. Different degrees of hydrolysis of PVA are obtainable and the different degree of hydrolysis is decisive with regards to the properties. The degree of hydrolysis corresponds to the amount of hydroxyl group incorporated in the polymer, which allows tuning of hydrophilicity/hydrophobicity of the polymer.[46] Hydrophobically modified PVA will be more amphiphilic, leading to increased surface and interfacial activities than hydrophilic PVA [47]. PVA is used in a range of application areas (paper industry,

textile industry, printing etc.). Nevertheless, PVA is most knowingly used as aid in pharmaceuticals and found in ophthalmic solutions in lubricants.[48]

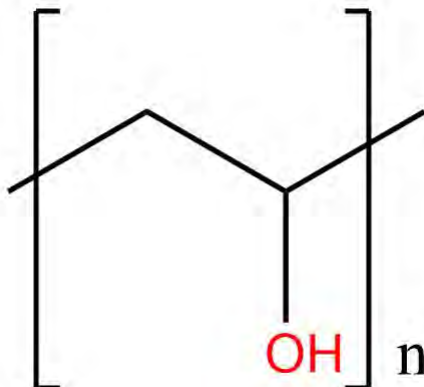


**Figure 2.12:** The molecular structure of polyvinyl alcohol (PVA).

## 2.7 Analytical techniques

During the course of the project, a number of instruments/techniques were employed to gain interpretable results. The three main analytical techniques utilized in the project were microscopy, optical tensiometry and nuclear magnetic resonance spectroscopy (NMR). When analyzing microcapsule morphology and constructing size distribution, bright field (light) and fluorescence microscopy were essential. Optical tensiometry and specifically the pendant drop method, is a technique employed for measurements of interfacial tension between liquids (see section 3.4.3 for the purpose of this project). NMR is utilized for characterization of chemical structure (see section 3.3.2 and section 3.4.1 for the purpose of this project). In this section, the analytical techniques utilized will be thoroughly outlined.

### 2.7.1 Bright field (light) & fluorescence microscopy

There are a wide range of microscopy techniques available. The overall principle of microscopy is to illuminate a specimen by electromagnetic radiation and with the use of lenses, attain a visible image.[49] Light microscopy is one of the more conventional techniques, due to the use of white light. One example of a light microscopy type is bright field microscopy. In bright field microscopy, the beam of light is passing by a condenser lens before hitting the specimen to focus the light onto the specimen. Light transmitted from the specimen will then pass an objective lens which will collect the light and form a magnified image. The advantage of bright field is its simplicity; it is one of the simplest optical microscopy types that exist. However, it is difficult to produce images with high contrast if the samples have low spatial resolution of the refractive index.[50] A schematic illustration of a bright field (light) microscopy is presented in figure 2.13.

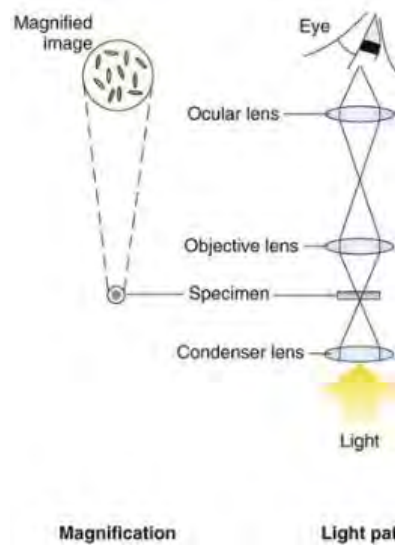


**Figure 2.13:** Schematic illustration of bright field microscopy. (Modified) [51]

Another type of microscopy technique is fluorescence microscopy. Instead of visible light, ultraviolet light is irradiated from the light source, which often is derived from a mercury or xenon lamp. Certain specimens (fluorophores) will emit light when irradiated with ultraviolet light [52]. The property of being fluorescence-active could be intrinsic or added to a specimen by treating it in fluorescent solutions [49]. A key characteristic of fluorescence microscopy is the filters employed. Two different filters are used, an excitation and a barrier filter. The excitation filter is positioned in front of the light source and ensures that the desired wavelength is hitting the specimen. The barrier filter is placed in line with the eyepiece and filters wavelengths that are not emitted by the fluorophores. The barrier filter will provides the advantage of a high signal-to-noise-ratio.[52] The setup is illustrated in figure 2.14.

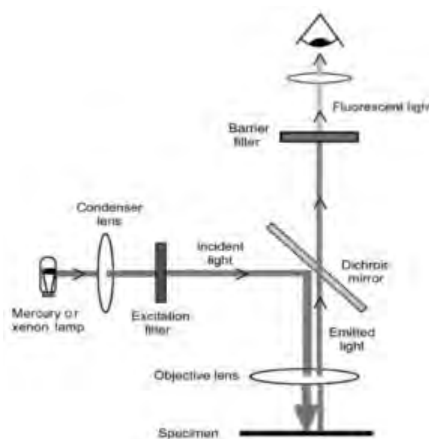


**Figure 2.14:** The setup of fluorescence microscopy. [52]

## 2.7.2 Interfacial tension & pendant drop method

The pendant drop method is a commonly used method to obtain information about interfacial tension between two immiscible liquids. A drop of one liquid is suspended vertically from the tip of a needle [53]. By analyzing the drop shape with an optical tensiometer, the interfacial tension could be derived from Young-Laplace equation (equation 2.3):

$$\gamma = \frac{g\rho(d_e)^2}{H} \quad (2.3)$$

The interfacial tension ( $\gamma$ ) relates to the gravitational forces ( $g$ ) and the capillarity forces. The factors affecting capillarity force acting upon the droplet are droplet density ( $\rho$ ), maximum droplet diameter ( $d_e$ ) and a correction factor ( $H$ ). The correction factor is included to take into account the influence of the form of the droplet. When applying the pendant drop method, there are assumptions made. For instance, it is assumed that the droplet is in equilibrium state, meaning there is no inertia that is affecting the form of the droplet during the actual measurement. This means that the gravitational and capillarity force are the only forces that affect the droplet. Furthermore, it is assumed that the droplet is symmetrical, meaning that the measurements are direction-independent.[54]

### 2.7.2.1 Gibbs adsorption isotherm

The relation between the surface concentration ( $\Gamma$ ) and the interfacial tension ( $\gamma$ ) of a surfactant is covered by Gibbs adsorption isotherm (equation 2.4).

$$\Gamma = -\frac{1}{nRT} \frac{\partial \gamma}{\partial \ln a} \quad (2.4)$$

The letter  $n$  is a factor that depends on the type of surfactant, where  $n$  equals one when nonionic surfactants are treated. For monovalent ionic surfactants,  $n$  equals two (surfactants that contains two species, one counterion and one surfactant). For divalent ionic surfactants,  $n$  equals three (two counterions and one surfactant ion). The activity of the surfactant  $a$  is in practise the concentration of the surfactant in the bulk solution.[45].

## 2.7.3 Nuclear Magnetic Resonance Spectroscopy (NMR)

Nuclear magnetic resonance spectroscopy (abbreviated to NMR), is a technique that exploit the fact that atomic nuclei have a characteristic *spin*. This property is associated with the magnetic moment of the atom(s). When applying a magnetic field, the intrinsic magnetic moment will change and a number of spin states will be generated. With a stronger applied magnetic field, the energy difference between the spin states increases. The energy difference is expressed according to equation 2.5.

$$\Delta E = \gamma \frac{h}{2\pi} B_0 = h\nu \quad (2.5)$$

## 2. Theory

---

The energy difference will depend on the magnetogyric constant  $\gamma$  and the strength of the magnetic field. Furthermore, the energy difference can be described as a function of the resonance frequency,  $\nu$ . Atomic nuclei will absorb energy (resonance) at different frequencies depending on the electronic environment. This feature provides the unique chemical selectivity (the high spectral resolution) of NMR. The frequency (spectral position) is known as the *chemical shift*. With NMR spectroscopy, characterization of chemical structure and the possibility of quantifying concentrations are enabled.[55]

# 3

## Methods

A literature study was conducted to establish a foundation for succeeding stages of the methodology. This step was followed by investigations of the solubility of the cationic antimicrobial compounds in the oils of interest. Microcapsule formulation through internal phase separation by solvent evaporation (see section 2.2) of the promising combinations were then conducted. To characterize morphology and size distribution of the promising systems, *bright field microscopy* and *fluorescence microscopy* were utilized. The software tool *ImageJ* was utilized to enhance the images and constructing size distributions. For the unpromising combinations, further development of active substance was conducted, see section 3.4.

### 3.1 Chemicals and Materials

The following chemicals were exploited during the course of the project:

- Poly(D,L-lactide-co-glycolide) 70:30,  $M_w \approx 10000$ , Polysciences, Inc. (19247)
- Ethyl linoleate,  $\geq 95.0\%$ , Sigma-Aldrich (L1751)
- Olive oil, Fluka BioChemicals (75348)
- Sunflower oil from *Helianthus annuus*, Sigma-Aldrich (S5007)
- Glyceryl trioctanoate,  $\geq 99.0\%$  Sigma-Aldrich (T9126)
- Glyceryl tributanoate, Sigma-Aldrich (T8626)
- Docosahexanoic acid methyl ester  $\geq 98.0\%$ , Cayman Chemical (10006865)
- Jojoba oil from *Simmondsia chinensis*, Sigma-Aldrich (59980)
- Benzylkonium chloride,  $\geq 95.0\%$ , Sigma-Aldrich (kod)
- Octenide dihydrochloride 97.0%, Ark Pharm (AK327325)
- Pyrene  $\geq 99.0\%$ , Sigma-Aldrich (82648)
- Poly(vinyl alcohol)  $\geq 95.0\%$  hydrolyzed,  $M_w \approx 95000$ , Acros Organics (A0254033)
- Dichloromethane, Sigma-Aldrich (L090000)
- Acetone,  $\geq 99.8\%$ , VWR Chemicals

Furthermore, Milli-Q-water was utilized throughout the project. The following materials, equipment and softwares were utilized during the course of the project:

- Hamilton syringe 1 mL model 81320
- Heidolph Silent Crusher homogenizer model M tool 6F
- UV Spectrophotometer HP8453
- 5 ml 14/10 round bottom flask with side neck, Ace Glass (9592-35)

- Zeiss Axio Imager 2
- NIH ImageJ
- MATLAB R2019b
- Biolin Scientific Optical Tensiometer, Software; OneAttension
- Varian MR 400 spectrometer (Palo Alto, CA)
- MestReNova version 12.0 (Mestrelab Research, Santiago de Compostela, Spain)

## 3.2 Solubility of active substances in core oils

A prerequisite for enabling encapsulation of core oil and active substance, is that the active substance is dissolved in the core oil. The active substances of interest were two different cationic antimicrobial substances, benzylnonium chloride and octenidine dihydrochloride. The solubility tests were conducted according to following procedure; the weight of an active substance was initially measured so it would constitute 0.1 weight-% of the active substance/oil-mixture. When the oil had been added, the sample was put on a stirring plate. The stirring was proceeded until dissolution was observed. The stirring was proceeded at most within 2-3 days. If the active substance was not dissolved, the saturation point was assumed to be at the current weight-% or less. If active substance was substantially dissolved, active substance was added so that it constituted 0.5 weight-%. This proceeded stepwise, until dissolution could not be observed.

To investigate the influence of heat and whether increasing the temperature will improve the solubility, samples containing 1 weight-% of active substance and 1:1-weight-ratio of dichloromethane/core oil were prepared. The samples were heated under influence of nitrogen gas. Flushing with nitrogen gas began at 35 °C and continued until 45 °C. The treatment with nitrogen gas was conducted to keep an inert environment for the core oil while evaporating dichloromethane. At 45 °C, the heat was turned off whereas the flushing with nitrogen gas remained. The samples were stirred with magnetic stirrers during the heating procedure.

## 3.3 Internal phase separation by solvent evaporation

To enable dissolution of the active substances into the core oils, the method of formulation developed by Loxley and Vincent [18] was altered. Dichloromethane was exchanged with chloroform to enable controlled evaporation at higher temperatures (50 °C), since the boiling point of chloroform is higher than that of dichloromethane.

### 3.3.1 Microcapsule formulation

The microcapsule formulations was based on previous work of Loxley and Vincent [18] and Eriksson [23]. All microcapsule formulations consisted of 1 wt% of active substance and 0.5 wt% pyrene. The continuous water phase was Milli-Q-water with

1 wt% of PVA. Due to the relatively small scale of the formulations and subsequently, the low amounts used for each formulation ( $\approx 0,33\text{mg}$  of QAC), a stock solution was prepared so that the actual microcapsule formulations would be feasible. From previous studies, a relatively high polymer:oil-ratio would induce formation of multi-core morphology rather than single-core morphology [23], hence a polymer:oil-ratio (based on weight) of 3:1 was chosen. Acetone was added to all formulations to stabilize and aid the emulsification process [18]. The recipe for the microcapsule formulation is presented in Table 3.1.

**Table 3.1:** The recipe for the microcapsule formulations.

Active substance (mg)	0.33
Pyrene (mg)	0.17
DCM (g)	2.91
PLGA (g)	0.1
Oil (g)	0.033
PVA-solution (ml)	6
Acetone ( $\mu\text{l}$ )	200

### 3.3.2 Characterization of microcapsules

The characterization of the microcapsules were conducted with bright field and fluorescence microscopy. *Zeiss Axio Imager 2* was the instrument utilized. The purpose of bright field microscopy was to assess the overall quality of the sample. The images obtained were treated with the software *ImageJ* in order to gain the size of microcapsules size for the systems of interest. Subsequently, *MATLAB R2109b* was employed to construct lognormal size distributions for the systems of interest. Fluorescence microscopy was mainly utilized to assess morphology. Fluorescence microscopy could only be utilized when a coloring agent was incorporated. Hence, pyrene was included in the microcapsule formulations. To characterize the partition of benzalkonium chloride between microcapsule and continuous aqueous phase, a sample was formulated with ethyl linoleate, 1 wt% benzalkonium chloride and a aqueous phase of heavy water ( $\text{D}_2\text{O}$ ) and 1 wt% PVA. The sample was characterized with NMR spectroscopy. Specifically, quantitative  $^1\text{H}$  NMR spectra were acquired using a Varian MR 400 spectrometer (Palo Alto, CA). Each spectrum was collected by 32-1024 acquisitions using a relaxation delay of 10 s and a 45 degree RF-pulse followed by a 3 s acquisition time with a 6410 Hz spectral width in the frequency domain. The experiments in this work were carried out at 25 °C. For the spectral analysis and integral calculations, the software program MestReNova version 12.0 (Mestrelab Research, Santiago de Compostela, Spain) was employed.

## 3.4 Deprotonated octenidine

Since salts are poorly soluble in oils, it was decided to investigate the possibilities of improving the solubility by developing a method to modify octenidine dihydrochloride into a hydrophobic derivative. Comparing with octenidine dihydrochloride,

the molecular structure of deprotonated octenidine (presented in Figure 3.1) will differentiate in two aspects. Firstly, the corresponding amin nitrogen in octenidine dihydrochloride is instead an imin nitrogen for the deprotonated compound. Secondly, the corresponding aromatic rings of octenidine dihydrochloride are not aromatic for deprotonated octenidine.

If sufficient solubility (1 wt% of the active substance) was not achieved, further studies were conducted to compare the surface activity-related properties of deprotonated octenidine with octenidine dihydrochloride. Microsphere formulation of deprotonated octenidine and interfacial tension measurements involving both deprotonated octenidine and octenidine dihydrochloride were conducted.

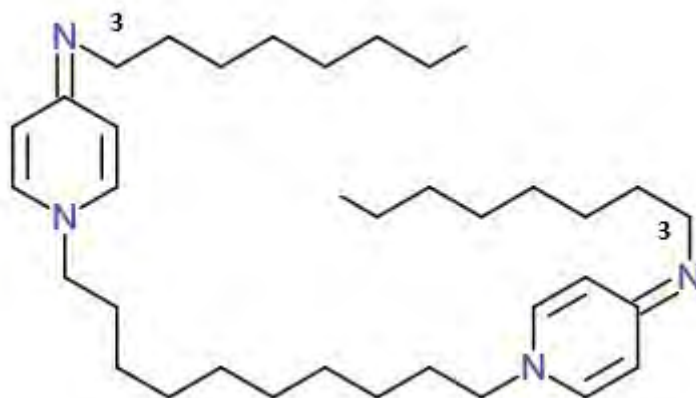


**Figure 3.1:** The molecular structure of deprotonated octenidine. The notion of (3) will be referenced in section 4.3.

#### 3.4.1 Deprotonation of octenidine dihydrochloride.

Octenidine dihydrochloride was dissolved in methanol, into which a sodium hydroxide (with a 2:1 octenidine dihydrochloride:sodium hydroxide molar ratio) dissolved in methanol was slowly added dropwise. The sample was then stirred in a fume hood for at least 12 hours so that all methanol could evaporate from the sample. Milli-Q-water was then added and the precipitate was centrifuged at 2000 rpm for 60 minutes. Vacuum filtration was then employed, to separate the sodium chloride from the deprotonated octenidine hydrochloride by washing with milli-Q-water. The centrifugation and the vacuum filtration was conducted in three rounds. Lastly, the sample was put in a fume hood for evaporation of residual water for at least 12 hours. To verify the conversion to deprotonated octenidine, NMR spectroscopy was employed.

### 3.4.2 Microsphere formulation of deprotonated octenidine

To investigate the formulation properties in relation to octenidine dihydrochloride, microspheres were formulated consisting of deprotonated octenidine. Internal phase separation by solvent evaporation was the method to formulate the microspheres. For all of the formulations, a continuous aqueous phase of 1 wt% PVA-solution were employed. Three formulations were conducted, which are presented in Table 3.2. The weight percent of deprotonated octenidine are in regards to the amount of polymer used in the formulations.

**Table 3.2:** The microsphere formulations involving encapsulation of deprotonated octenidine.

Deprotonated octenidine (wt%)	DCM (g)	PLGA (g)	Acetone ( $\mu$ l)
0	2.65	0.1	200
5	2.78	0.1	200
10	2.92	0.1	200

### 3.4.3 Interfacial tension measurements of octenidine dihydrochloride and deprotonated octenidine

The pendant drop method was utilized using an *optical tensiometer* to further investigate the surface activity-related properties of the deprotonated octenidine in relation to octenidine dihydrochloride. The samples were prepared according to the methodology applied in a previous study [56]. In contrast to the microsphere formulations, a continuous aqueous phase consisting 5 wt% PVA-solution were utilized. The samples were prepared by dissolving the compounds in different amounts in dichloromethane. The weight percent of active substance are in regards to the polymer (0.1 g PLGA) in the microencapsulation formulation rather than the amount of dichloromethane used in the sample preparation. For the samples with a low amount of active substance (0.025 and 0.25 wt%), a stock solution of the active substances and dichloromethane was prepared to enable dilution of those samples. For each sample, 7 measurements were conducted. An average was calculated of all of the data points (interfacial tension) and collected for each sample. The samples are presented in Table 3.3. From the data obtained, the surface concentration for both compound are calculated with equation 2.4.

### 3. Methods

---

**Table 3.3:** The samples for interfacial tension measurements. The stock solution contained 0.0025 g of active substance and 10 g of dichloromethane (0.33 mg/ml).

Active substance (wt%)	Stock solution (g)	DCM (g)	Active substance (g)
0	-	2.65	-
0.025	0.1	2.55	-
0.25	1	1.65	-
2.5	-	2.71	0.0025
3.3	-	2.74	0.0033
4.2	-	2.76	0.0042
5	-	2.78	0.0050
7.5	-	2.85	0.0075
10	-	2.91	0.0100
12.5	-	2.98	0.0125
15	-	3.05	0.0150

# 4

## Results & Discussion

In this section, the solubility of the active substances in the oils of interest will be outlined. Thereafter, the microcapsule formulation of promising systems will be presented. Finally, the studies regarding the modified (deprotonated) octenidine will be presented.

### 4.1 Solubility of cationic antimicrobial surfactans in biocompatible oils

The solubility of benzalkonium chloride in the tested oils are presented in Table 4.1.

**Table 4.1:** Solubility of benzalkonium chloride in biocompatible oils.

Oils	Dissolvable concentration (wt-%)
Ethyl linoleate	<1
Glyceryl tributanoate	0.1
Glyceryl trioctanoate	<0.1
Olive oil	<0.1
Sunflower oil	<0.1
Docosahexanoic acid methyl ester	1
Jojoba oil	0.1

The dissolution was low across all the tested oils. Since benzalkonium chloride is a salt, dissolution into nonpolar solvents is slow. Yet, there were an observable difference between some of the oils. Notably, highest benzalkonium chloride dissolution was achieved with ethyl linoleate and docosahexanoic acid methyl ester, whereas the lowest dissolution were achieved with glyceryl trioctanoate, olive oil and sunflower oil. Since benzalkonium chloride is readily dissolvable in water, it will be more prone to dissolve in aprotic oils rather than nonpolar oils.

Regarding octenidine dihydrochloride, the dissolution was lower across all oils. 0.1 wt% could not be dissolved in any oil. Likewise with benzalkonium chloride, octenidine dihydrochloride is a salt and dissolves poorly in nonpolar solvents.

### 4.1.1 Solubility & influence of heat

Due to the low solubility of the active substances, a modified solubility test involving heat were conducted. The findings are presented in Table 4.2.

**Table 4.2:** The solubility tests involving heat treatment. The star (\*) indicate systems which became opaque after the tests and actual confirmation of solubility.

Oils	Dissolution of BAC at 1wt%	Dissolution of OCT at 1wt%
Ethyl linoleate	YES*	NO
Glyceryl tributanoate	YES	NO
Glyceryl trioctanoate	YES*	NO
Olive oil	YES	NO
Sunflower oil	YES	NO
Jojoba oil	YES	NO

The dissolution were significantly improved for the benzalkonium chloride systems than for the corresponding octenidine dihydrochloride systems. However, there are nuances that should be taken into account. Immediately after the heating procedures were conducted, both ethyl linoleate and glyceryl trioctanoate displayed dissolution, which strengthens the hypothesis of increasing the temperature will improve the solubility. However, both systems became opaque with time (\*). Still, both systems are categorized as soluble for benzylkonium chloride. Difficulties were encountered when separating dichloromethane and the jojoba oil. The jojoba oil became hardened after the heating procedure. An explanation for the hardened jojoba oil could derive from the low volatility and the treatment with nitrogen gas. When treating the sample with nitrogen gas, the jojoba oil at the vicinity of the nitrogen gas will become cooler than the jojoba oil at the bottom of the sample. Since jojoba oil has a freezing point of 7.0-10.6 C (see section 2.4.3), there will be a local cooling and hardening of the jojoba oil. Besides the aforementioned systems, dissolution was achievable for the other benzalkonium chloride systems. Microcapsule formulation according to the procedure outlined in section 3.3.1 was subsequently conducted for all systems involving benzalkonium chloride.

Regarding the systems involving octenidine dihydrochloride, phase separation was observed before the heat treatment for glyceryl tributanoate and glyceryl trioctanoate, olive oil and sunflower oil became instead phase separated during the heating procedure. For the jojoba oil, a dense foam was formed during the heat treatment. The explanation for the hardening of corresponding benzylkonium chloride sample could be applied in this case. The ethyl linoleate system became opaque before the heating procedure and remained opaque after the heating procedure. Due to the inability to dissolve in the oils even when heat was introduced, the compound had be modified to become more hydrophobic (section 4.3).

## 4.2 Microcapsule formulation: Benzalkonium chloride

In Table 4.3, the morphology are presented for each system involving benzalkonium chloride. For five of the systems (ethyl linoleate, glyceryl trioctanoate, olive oil, sunflower oil and DHA), core-shell morphology were enabled. For the jojoba oil, a mixture of acorn and core-shell particles could be observed. Glyceryl tributanoate did not form any microcapsules [57]. In this section, the appearance of the microcapsules for the benzalkonium chloride systems are presented and discussed. Furthermore, the size distribution for each system will be outlined.

**Table 4.3:** Observed morphology for systems involving 1wt% benzalkonium chloride.

Oil	Morphology
Ethyl linoleate	Core-Shell
Glyceryl tributanoate	Droplet separation
Glyceryl trioctanoate	Core-shell
Olive oil	Core-shell
Sunflower oil	Core-shell
Docosahexanoic acid methyl ester	Core-shell
Jojoba oil	Acorn/Core-shell

### 4.2.1 Core-shell systems

With ethyl linoleate, glyceryl trioctanoate, olive oil, sunflower oil and DHA as core oil, core-shell morphology was attained, see Figure 4.1 for the illustration for the case of ethyl linoleate and Appendix A for the other oils. Besides the morphology, non-central cores was observed for all core-shell microcapsule systems. The appearance of non-central cores could indicate a slightly poorer wetting between oil and polymer than the ideal case when the cores are central. A distinguishing factor from the method of formulation in this project and the method of formulations employed by Loxley/Vincent and Eriksson are the input of heat during the evaporation of the volatile solvent (chloroform in this project). With the only exception of glyceryl trioctanoate, all of the oils were to some extent unsaturated. Since the evaporation did not occur in vacuum conditions, there is a possibility for the oils to become more saturated. If that is the case, the wetting abilities between oil and polymer will differentiate from when heat treatment is not employed. However, the observations of non-central cores has been made for equivalent systems where heat treatment is not employed [57]. In addition, this explanation does not account for the appearance of non-central cores when encapsulating the saturated glyceryl trioctanoate.

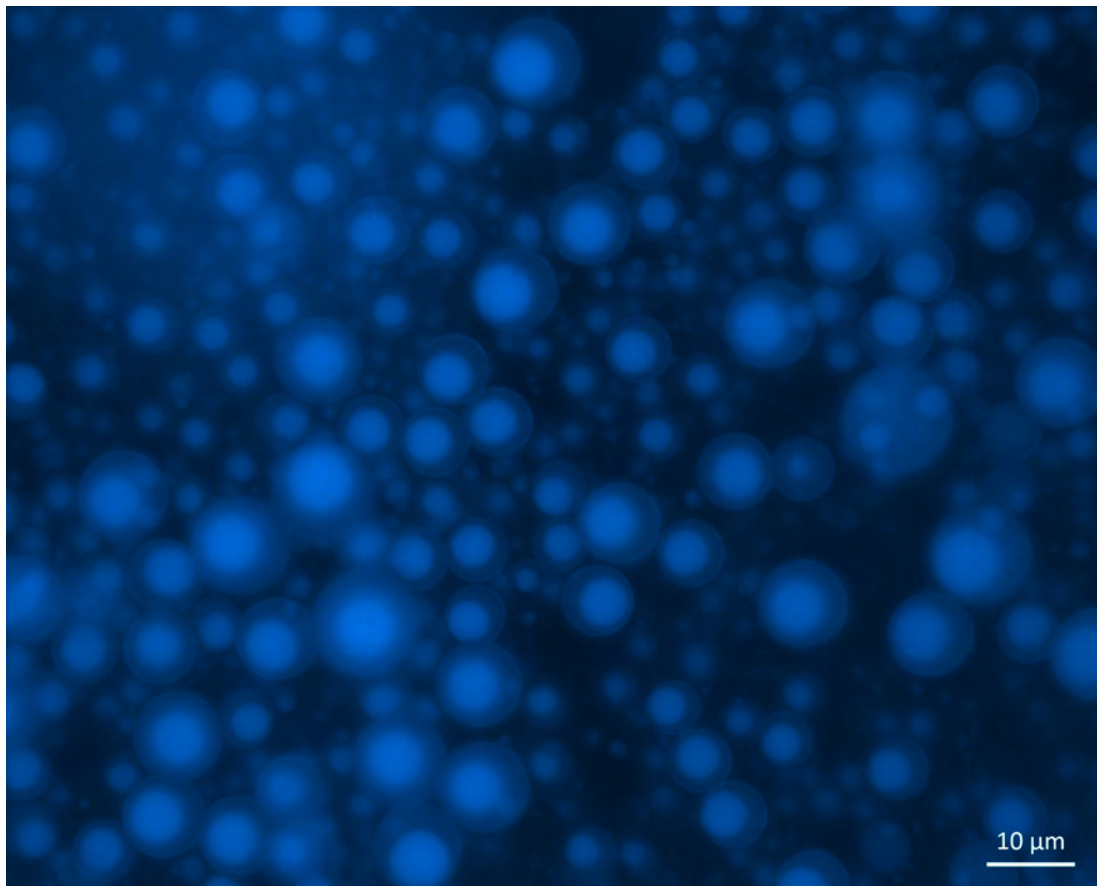


**Figure 4.1:** Microcapsules with ethyl linoleate observed with fluorescence microscopy (100x magnification).

In contrast to the other core-shell microcapsule systems, docosahexanoic acid methyl ester (DHA) generated capsules with significantly larger cores (see Figure 4.2). Unlike the other oils, docosahexanoic acid methyl ester was dissolved in an ethanol solution when handled. Consequently, a greater amount of the ethanol/docosahexanoic acid methyl ester solution had to be accommodated to attain the amount of oil desired. A potential consequence of this is more oil is included than planned. However, since the oil is dissolved in ethanol, it should be evenly distributed. Another potential explanation for the appearance of larger cores is the ethanol being encapsulated together with the oil. Pyrene dissolves in ethanol and will not distinguish between oil/ethanol when observing the microcapsules in fluorescence microscopy. However, when the evaporation of volatile solvent was conducted, it was ensured that the final weight of the sample only accounted for the actual oil, continuous aqueous phase, polymer and active substance.

Furthermore, non-central cores could be observed. A possible explanation derives from the the unsaturated nature of DHA. The oil consists of six double bonds, making it susceptible for oxidation. It is therefore probable that oxidation occurred and the wetting ability with PLGA was altered. However, as mentioned in section 4.2.1, the appearance of non-central cores could be observed for the saturated glyceryl trioctanoate.

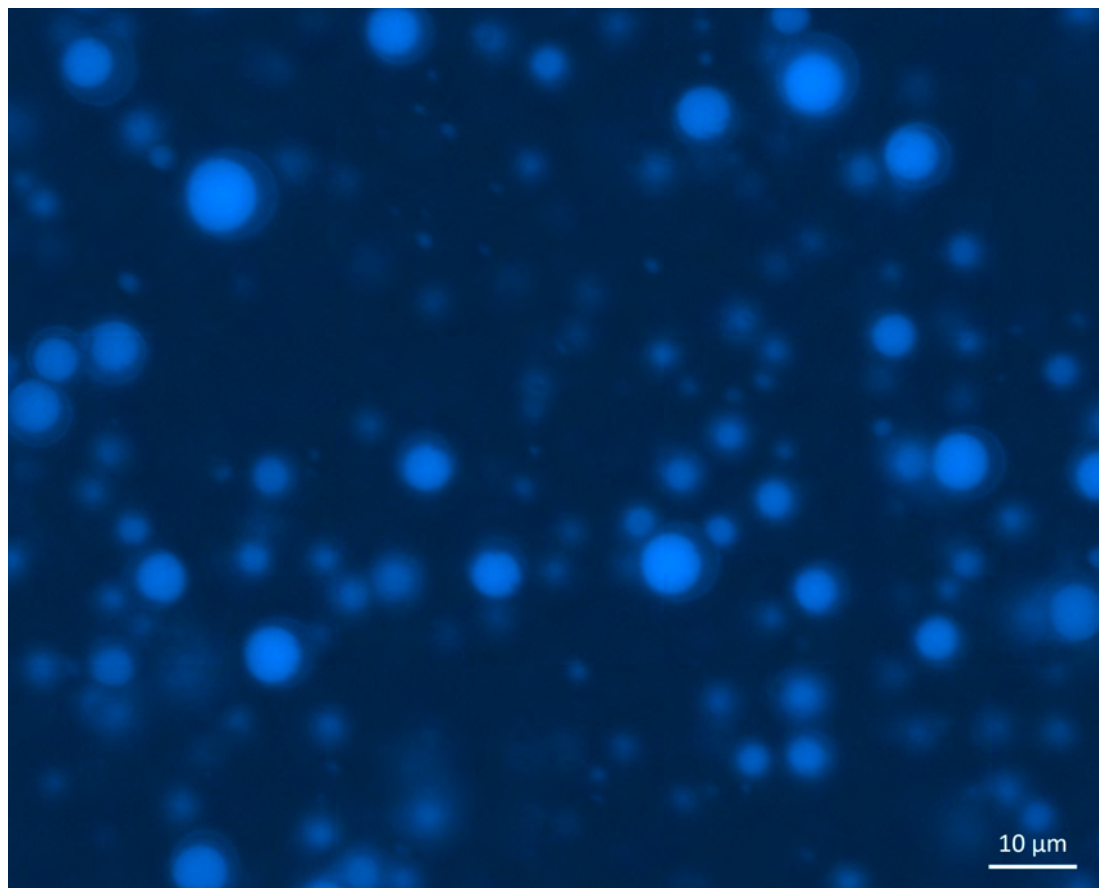


**Figure 4.2:** Microcapsules with docosahexanoic acid methyl ester observed with fluorescence microscopy (100x magnification).

#### 4.2.2 Size distributions of core-shell microcapsules

Size distributions that were constructed from bright field microscopy images are presented in Figure 4.3. Overall, the size distributions were similar with small deviations between the systems. The observed deviations could be explained by difficulties to attain identical formulation procedure. Initially, when all of the ingredients are added to the round bottom flask, a phase separation will occur. Mixing the emulsion is conducted, nevertheless the mixing will deviate between formulations. Another explanation for the observable deviations between the systems is due to the software utilized for the construction of size distributions, *ImageJ*. The software itself is unable to identify and differentiate microcapsules from oil droplets, broken polymer fragments and so on. The process from attained images in bright field microscopy to constructed size distributions was conducted manually, by contrasting identified microcapsules from the background of the bright field microscopy images. However, these explanations do not fully account for the two systems that deviated the most, olive oil and sunflower oil. For those particular systems, the size distributions are broadened and the peaks are shifted.

As mentioned in section 2.4.6 and 2.4.7, both oils are a mixture of triglycerides. Triglycerides are both relatively large molecules and unsaturated, making the molar-

ratio of PLGA:olive oil/sunflower oil larger than any of the other oils and relatively prone for oxidation during the evaporation process. These factors allows alteration of the interfacial properties of the oil to a more significant degree than the other oils of interest. However, it should be emphasized that the source of error derived from the acquisition of the microcapsule sizes from *ImageJ* has a larger impact, since the visual appearance of the olive oil and sunflower oil microcapsules (for images, see Appendix A) did not differentiate significantly from the other core-shell systems.

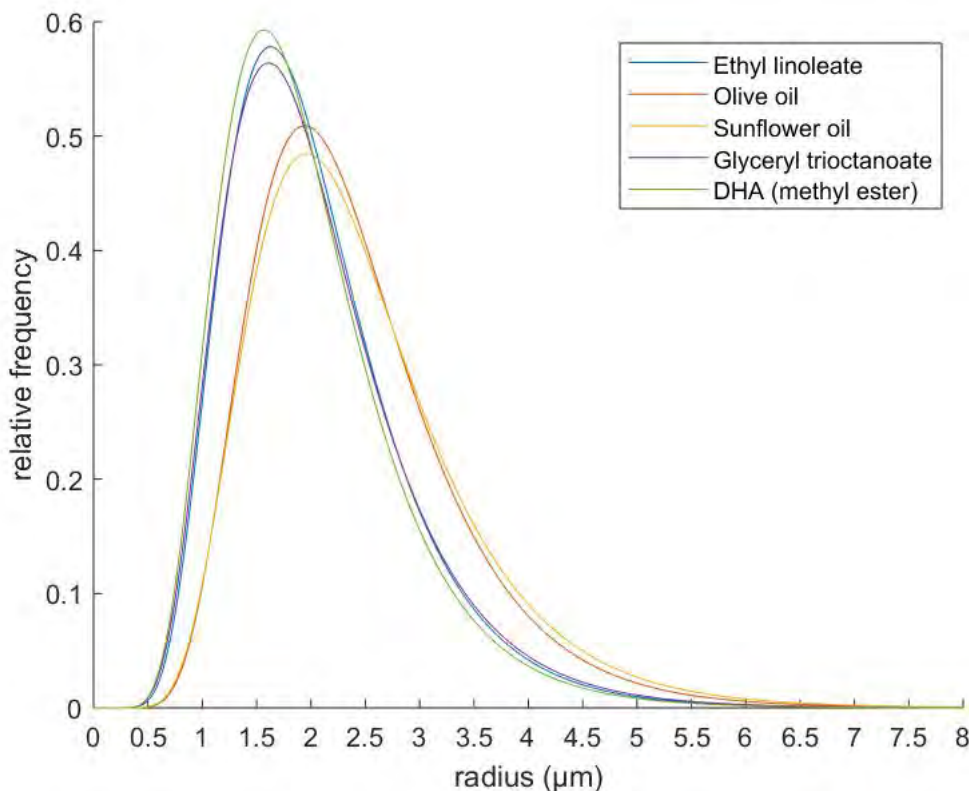


**Figure 4.3:** Size distributions of all core-shell systems involving benzalkonium chloride with a lognormal fitting.

### 4.2.3 Jojoba oil

Jojoba oil was the only oil exhibiting two different morphologies, namely acorn and core-shell. Figure 4.4 demonstrate the appearance of acorn shaped microcapsules. By comparing the spreading coefficients which enables core-shell and acorn morphology, it is evident that the difference between these morphologies is the sign of the spreading coefficient of the polymer ( $S_P$ ), where its negative for acorn and positive for core-shell morphology. These results could indicate that jojoba oil have a poorer wetting ability with PLGA than the other oils. Since jojoba oil is a natural product which constitute of a mixture of fatty acid esters of different alkyl chain lengths, the wetting could be significantly reduced in comparison with purer fatty acid esters (e.g. ethyl linoleate). However, this explanation does not account the lack of acorn

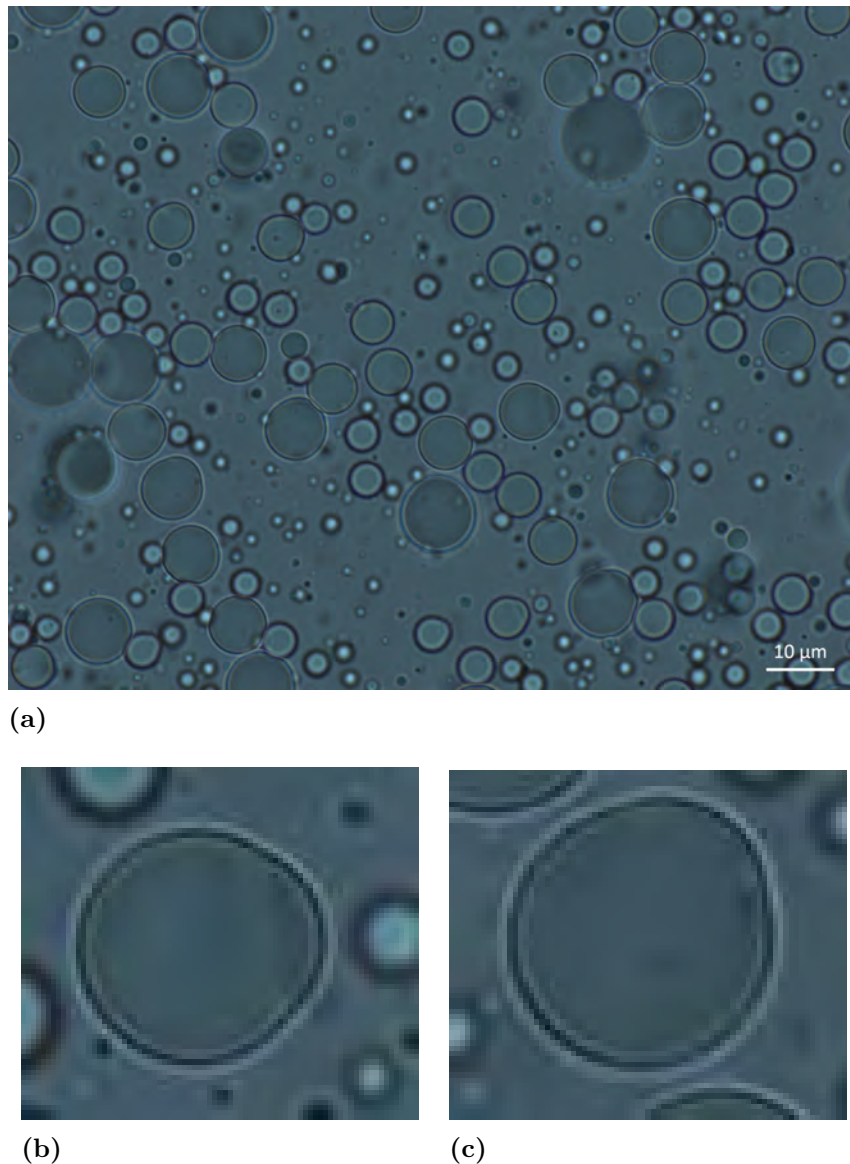


**Figure 4.4:** Microcapsules with jojoba oil observed with bright field microscopy (100x magnification), where (b) and (c) highlights the appearance of acorn.

microcapsules for olive oil and sunflower oil, which both are natural products which mainly constitute of a mixture of triglycerides. Another possible explanation for this behaviour derives from the formation of microcapsules from emulsion droplet. When the volatile solvent (chloroform) evaporates, the polymer (PLGA) will phase separate within the emulsion droplet. A possible state between dispersed polymer in emulsion droplets and core-shell particles is the formation of acorn between polymer (PLGA) and the oil. As indicated in section 4.1.1, it was particular difficult to evaporate dichloromethane from jojoba oil due to its low volatility. A similar effect could be evident during the formation of microcapsules, where jojoba oil required more time of heating to form core-shell microcapsules.

#### 4.2.4 Partition of benzalkonium chloride between microcapsules and aqueous phase

The distribution of benzalkonium chloride between microcapsules and the continuous aqueous phase was characterized using NMR spectroscopy. The NMR spectra presented in Figure 4.5 illustrate no detected presence of benzalkonium chloride in the continuous aqueous phase. Since benzalkonium chloride is the only compound in the encapsulation sample with aromatic rings, a signal at  $\sim 7.3$  ppm (1) could be expected if the compound was not encapsulated. As expected, a signal at  $\sim 7.3$  ppm could be identified for the reference sample. In comparison with the reference sample, no signal could be identified at  $\sim 7.3$  ppm for the encapsulation sample. When the NMR-spectra were superimposed at  $\sim 7.3$  ppm for both samples (Figure 4.6), the lack of signal for the encapsulated sample becomes evident. These results suggests that benzalkonium chloride was encapsulated when conducting the modified version of internal phase separation by solvent evaporation. Furthermore, these results contrasts from other studies relating to microencapsulation of benzalkonium chloride in microspheres [56], where no benzalkonium chloride was encapsulated. It should be emphasized that an modified method of formulation was employed in this case, where the organic solvent was chloroform instead of dichloromethane and the evaporation process was conducted at elevated temperatures (50 °C). The explanation for improved encapsulation is mostly due to the input of energy (heat), where there will be an increasing driving force towards dissolution of benzalkonium chloride in the oil (see solubility tests in section 4.1.1) and consequently, incorporation of benzalkonium chloride into the the PLGA microcapsules. However, it should be noted that since the amount of benzalkonium chloride used for the sample was low (0,33 mg), several scans had to be employed. Consequently, the signal-to-noise-ratio was low ( $\sim 3.40$ ), which implies a qualitative uncertainty in the results.

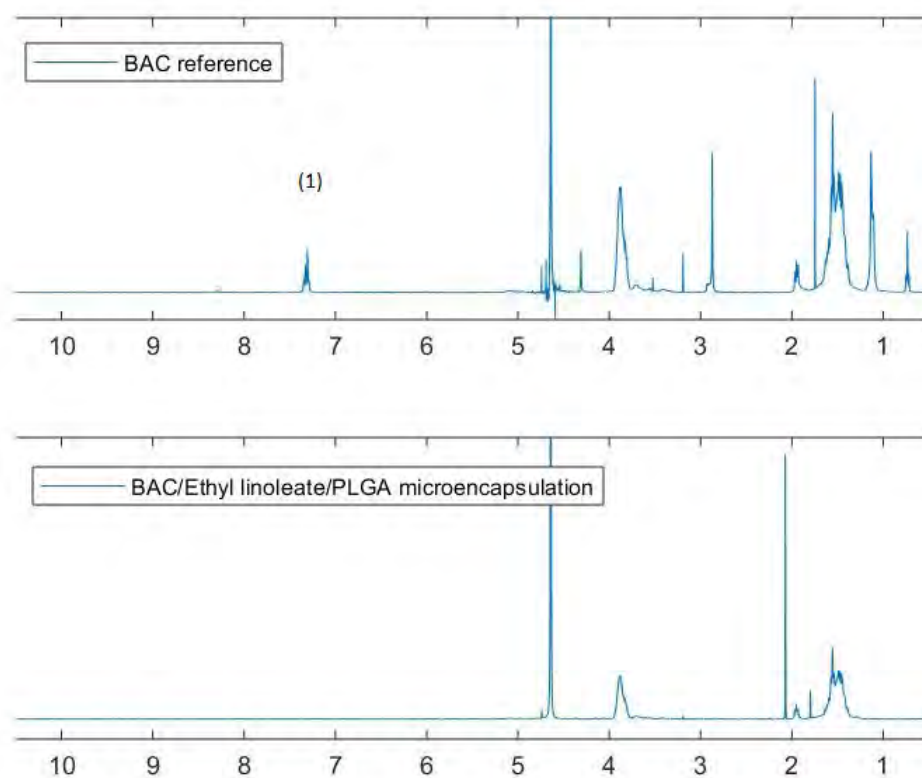


**Figure 4.5:** NMR spectra for reference sample with benzalkonium chloride and heavy water (upper image) and benzalkonium chloride encapsulated with ethyl linoleate in PLGA microcapsules (lower image). Milli-Q-water was exchanged with heavy water in the aqueous phase. The chemical shift (ppm) at the x-axes. The signal at (1) correspond to the aromatic ring in benzalkonium chloride, see Figure 2.10.

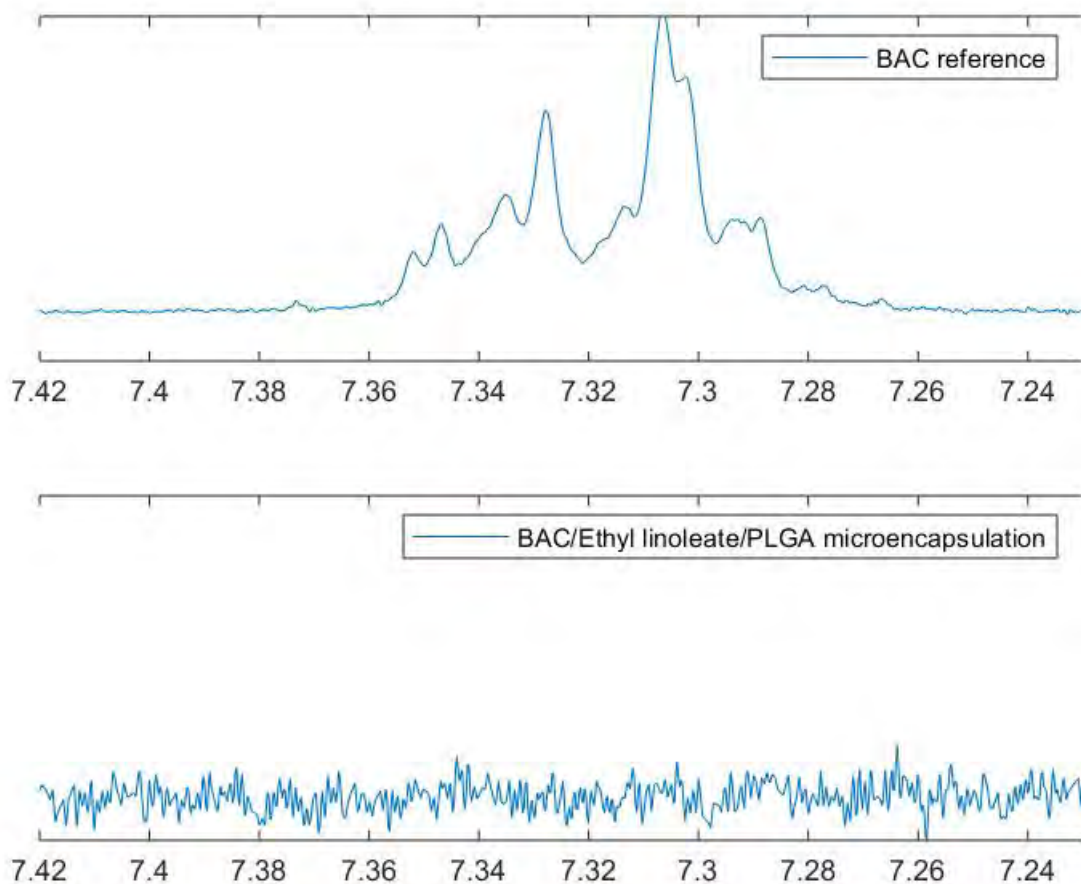


**Figure 4.6:** Superimposed NMR spectra in the 7.23-7.42 ppm range for reference sample with benzalkonium chloride and heavy water (upper image) and benzalkonium chloride encapsulated with ethyl linoleate in PLGA microcapsules with heavy water as aqueous phase (lower image). The chemical shift (ppm) at the x-axes.

### 4.3 Deprotonation of octenidine dihydrochloride

The yield of deprotonated octenidine was calculated to be 31 %. For calculations of yield, see appendix B. As indicated, the yield was relatively low. A significant source of error derives from the vacuum filtration and the fact that octenidine dihydrochloride has demonstrated solubility in water [56]. If the compound/water does not go through filter paper and rather ends at the bottom of the *Büchner funnel* through the sides of the filter paper, the vacuum filtration becomes ineffective. However, to verify the quality of the vacuum filtration, the filtrated water was filtered by vacuum filtration. This particular filtration yielded virtually no solid product, even though precipitate could be observed in the container, see Figure 4.7. An explanation for this occurrence could derive from the surface active properties of the compound and consequently, the ability to form micelles. By self-associating as micelles, the

dissolution will be improved, which will lead to a less effective vacuum filtration. However, this explanation does not fully account for the appearance of aggregates after the vacuum filtration (Figure 4.7).



**Figure 4.7:** The state of the filtered water after vacuum filtration.

The verification of deprotonated octenidine was conducted by nuclear magnetic resonance spectroscopy (NMR). The spectra for the deprotonated octenidine and octenidine dihydrochloride are presented in Figure 4.8. There are two signals in which octenidine dihydrochloride distinguishes itself from the deprotonated compound. The signal at  $\sim 10$  ppm corresponds to the proton bonded to the amine nitrogen ((2) in Figure 2.11 for octenidine dihydrochloride and Figure 3.1 for deprotonated octenidine). The signal is apparent for octenidine dihydrochloride. For the supposed deprotonated compound, there is no signal at  $\sim 10$  ppm. This indicates that deprotonation has occurred. The signal at  $\sim 3.2$  ppm ((3) in Figure 2.11 for octenidine dihydrochloride and 3.1 for deprotonated octenidine) for both spectra supports the interpretation at  $\sim 10$  ppm. The signal at  $\sim 3.2$  ppm corresponds to the proton(s) bonded to the carbon next to the amine nitrogen for octenidine dihydrochloride and imine nitrogen for deprotonated octenidine. From now and forward, that particular carbon will be referred to as the  $\alpha$ -carbon. For octenidine dihydrochloride, a quartet could be observed. The quartet derives from the coupling with three other protons; the protons bonded to the amine nitrogen and two protons bonded to the

carbon next to the  $\alpha$ -carbon. In the case of the deprotonated compound, a triplet could be identified at  $\sim 3.2$  ppm, implying that the particular proton is only coupling with two other protons bonded to the carbon next to the  $\alpha$ -carbon. These observations strongly indicates that deprotonated octenidine dihydrochloride was successfully achieved.

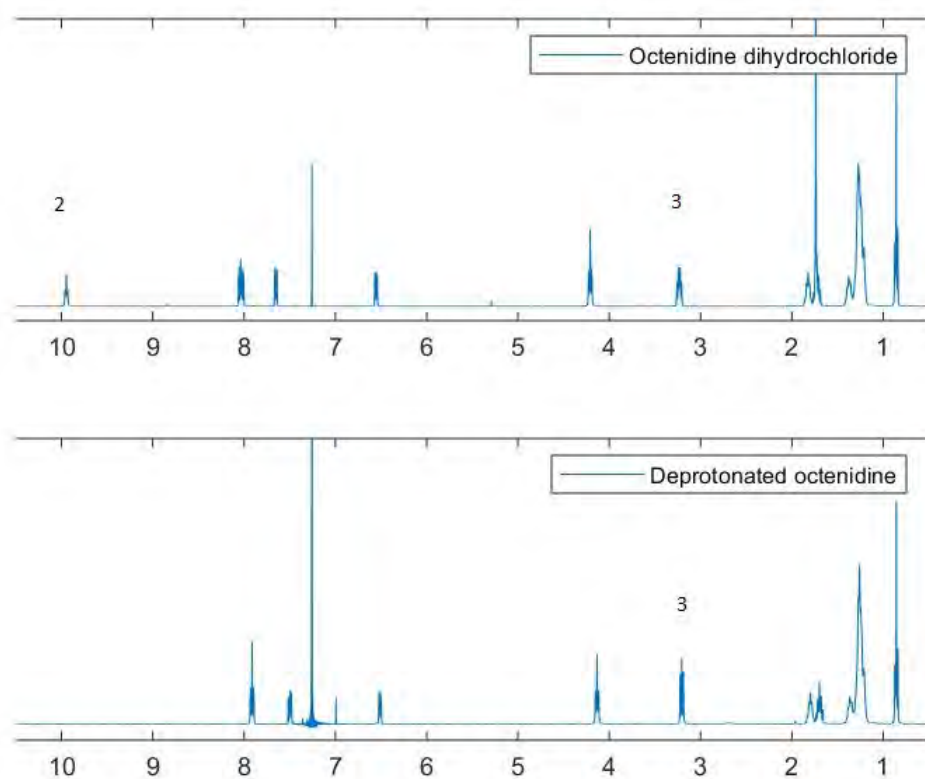


**Figure 4.8:** NMR spectra for octenidine dihydrochloride (upper image) and deprotonated octenidine dihydrochloride (lower image). The chemical shift (ppm) at the x-axis. The signals at (2) and (3) correspond to significant signals for octenidine dihydrochloride and deprotonated octenidine. Corresponding protons are illustrated in Figure 2.11 for octenidine dihydroachloride and Figure 3.1 for deprotonated octenidine.

### 4.3.1 Microsphere formulation of deprotonated octenidine

In Figure 4.9, the three different formulations involving deprotonated octenidine are presented. When increasing the amount of deprotonated octenidine, it was evident that the microspheres became overall smaller. This illustrates that, likewise with octenidine dihydrochloride, deprotonated octenidine is surface active [56]. However, it should be noted that these results do not illustrate whether there is a significant difference regarding interfacial tension between the active substances and the polymer (PLGA) interface.

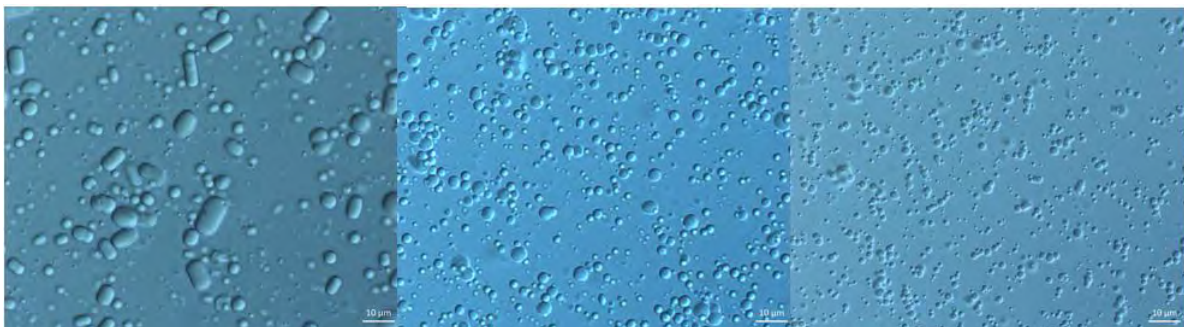


**Figure 4.9:** Microspheres with deprotonated octenidine observed in microscopy, with 0 wt% of deprotonated octenidine at the left, 5 % deprotonated octenidine represented in the middle and 10 wt% deprotonated octenidine at the right. 100x magnification for all images.

### 4.3.2 Interfacial tension measurements of octenidine dihydrochloride and deprotonated octenidine

The interfacial tension for the compounds and the relation to the logarithmic bulk concentration are presented in Figure 4.10. Detailed information about the measured interfacial tension with regards to the fraction of octenidine dihydrochloride and the modified compound is presented in Appendix C. What is observed is that the difference between the compounds are virtually within the margin of error. Hence, there is no significant difference in surface activity between octenidine dihydrochloride and the deprotonated compound. The reason for the resembling surface activity is derived from the stability in a broad pH-range (1.6-12.2) and the  $pK_a$  of 10.89 in which octenidine dihydrochloride exhibits. At a pH below of 10.89 (which is the case with PVA-solution employed for the interfacial tension measurements), octenidine dihydrochloride will remain protonated, whereas deprotonated octenidine will rather become protonated.

Furthermore, it is noticeable that the interfacial tension for the octenidine dihydrochloride is marginally lower than that for deprotonated octenidine. A possible explanation for the marginal difference is due to the salt (hydrochloric acid species) incorporated in the octenidine dihydrochloride and its potential influence on the interfacial tension. As mentioned in section 2.6, the presence of counterions will decrease the electrostatic repulsion between the octenidine units, consequently decreasing the interfacial tension. When octenidine dihydrochloride is deprotonated, there is an absence of counterions that decreases the electrostatic repulsion. Hence, deprotonated octenidine will lower the interfacial tension to a lesser extent than octenidine dihydrochloride.

The surface concentration for deprotonated octenidine and octenidine dihydrochloride are presented in Table 4.4. The results suggests that deprotonated octenidine was more densely packed at the surface than octenidine dihydrochloride, even when it is assumed to be charged ( $n=3$ ,  $\Gamma=1341$ ). However, there is no significant difference between the calculated surface concentrations when both compound are

assumed to be charged ( $n=3$ ), which corresponds with previous investigation of surface activity properties in terms of microsphere formulations and interfacial tension measurements. If deprotonated octenidine is assumed to be nonionic ( $n=1$ ), a significant difference could be observed regarding the calculations. However, this assumption does not account for the similarities in terms of surface activity for both compounds. Although the NMR spectroscopy suggested that a clean deprotonated compound was obtained, it is possible that not all of the octenidine dihydrochloride was converted. If that is the case, the model described in section 2.7.2.1 is not completely ideal in this particular case regarding the deprotonated compound.

**Table 4.4:** The Gibbs adsorption isotherm for deprotonated octenidine and octenidine dihydrochloride. The parenthesis is the isotherm for deprotonated octenidine if the compound is assumed to be uncharged ( $n=1$ ).

Active substance	$\Gamma(\text{\AA}^2/\text{molecule})$
Deprotonated octenidine	1341 (447)
Octenidine dihydrochloride	1435

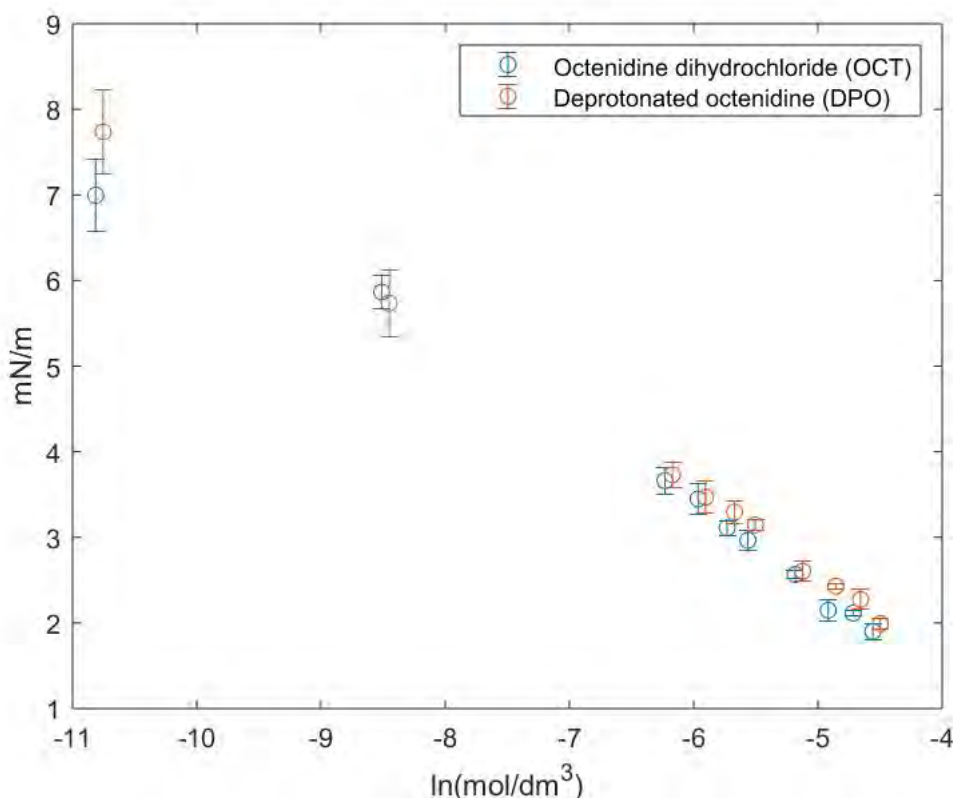


**Figure 4.10:** The interfacial tensions of octenidine dihydrochloride and deprotonated octenidine as a function of logarithmic bulk concentration.

# 5

## Conclusion

The low solubility of benzalkonium chloride and octenidine dihydrochloride in (bio-compatible) oils is a major problem which could be improved for benzalkonium chloride by supplying energy in terms of heat or mechanical energy (stirring). However, these measurements did not generate any promising results for octenidine dihydrochloride or for deprotonated octenidine.

NMR spectroscopy indicated that the developed method for deprotonation of octenidine dihydrochloride enabled the desired product. However, since the yield was relatively low (31 %), the method could be optimized in future studies of deprotonated octenidine.

It was evident that core-shell microcapsules were enabled when ethyl linoleate, glyceryl trioctanoate, olive oil, sunflower oil and docosahexanoic acid methyl ester were encapsulated along with benzalkonium chloride (1 wt%). Docosahexanoic acid methyl ester had substantially larger cores than the other core-shell systems. For jojoba oil, a mixture of core-shell and acorn microcapsules were formed whereas droplet separation occurred for glyceryl tributanoate. A general feature of the microcapsule were non-central cores. The reason for this behaviour has not been settled. Therefore, it is recommended to investigate further the mechanism of core-shell microcapsule formation and potential factors which leads to the consistent occurrence of non-central cores.

NMR spectroscopy suggested that a significant amount of benzalkonium chloride was successfully encapsulated, at least for the case ethyl linoleate being the core oil. However, NMR spectroscopy could not conclude the distribution of benzalkonium chloride within the capsules (between oil and PLGA). Therefore, it is recommended for future studies to investigate the distribution of benzalkonium chloride within the microcapsules. A suggested technique for investigating the distribution of benzalkonium chloride within microcapsules is Raman microscopy.

The size distributions for the core-shell systems were relatively similar, where olive oil and sunflower oil deviated more than rest of the systems. Both oils generated slightly broader size distributions and shifted peaks in contrast to the other oils. Both oils are an mixture of triglycerides and relatively unsaturated. When heat is introduced during the evaporation process, their interfacial properties could have been significantly altered. However, the error source derived from the processing of microscopy images was assessed to have a larger impact for the noticeable deviations.

## 5. Conclusion

---

In the comparative studies between octenidine dihydrochloride and deprotonated octenidine, it was evident that it was no considerable difference in terms of solubility and surface activity. This is due to the stability of octenidine dihydrochloride in a broad pH-range. For future studies, it is recommended to investigate further the properties of deprotonated octenidine. This includes studies regarding its suitability as an antiseptic agent for the purpose of treating non-healing chronic wounds.

# Bibliography

- [1] Robert Nunan, Keith G. Harding, and Paul Martin. “Clinical challenges of chronic wounds: searching for an optimal animal model to recapitulate their complexity”. In: *Disease Models Mechanisms* 7.11 (2014), pp. 1205–1213. DOI: 10.1242/dmm.016782.
- [2] Sbu, Swedish Agency for Health Technology Assessment, and Assessment of Social Services. *Svårläkta sår hos äldre - prevention och behandling*. Aug. 2014. URL: <https://www.sbu.se/sv/publikationer/SBU-utvarderar/svarlakta-sar-hos-aldre---prevention-och-behandling/>. (accessed: 02.15.2019).
- [3] J. P. Boyle et al. “Projection of Diabetes Burden Through 2050: Impact of changing demography and disease prevalence in the U.S.” In: *Diabetes Care* 24.11 (2001), pp. 1936–1940. DOI: 10.2337/diacare.24.11.1936.
- [4] Harold Brem and Marjana Tomic-Canic. “Cellular and molecular basis of wound healing in diabetes”. In: *Journal of Clinical Investigation* 117.5 (2007), pp. 1219–1222. DOI: 10.1172/jci32169.
- [5] Erik Gullberg et al. “Selection of Resistant Bacteria at Very Low Antibiotic Concentrations”. In: *PLoS Pathogens* 7.7 (2011). DOI: 10.1371/journal.ppat.1002158.
- [6] Megan C. Jennings, Kevin P. C. Minbiole, and William M. Wuest. “Quaternary Ammonium Compounds: An Antimicrobial Mainstay and Platform for Innovation to Address Bacterial Resistance”. In: *ACS Infectious Diseases* 1.7 (2015), pp. 288–303. DOI: 10.1021/acsinfecdis.5b00047.
- [7] Rob Atkin et al. “Preparation of Aqueous Core/Polymer Shell Microcapsules by Internal Phase Separation”. In: *Macromolecules* 37.21 (2004), pp. 7979–7985. DOI: 10.1021/ma048902y. (accessed: 02.14.2019).
- [8] Jonatan Bergek. *Evaluation of biocide release from modified microcapsules*. Doktorsavhandlingar vid Chalmers tekniska högskola. Ny serie: 4205. Chalmers University of Technology, 2017. ISBN: 9789175975245.
- [9] M. N. Singh et al. “Microencapsulation: A promising technique for controlled drug delivery”. In: *Research in pharmaceutical sciences* 5.2 (2010), pp. 65–77.
- [10] “REGULATION (EU) No 528/2012 OF THE EUROPEAN PARLIAMENT AND OF THE COUNCIL of 22 May 2012 concerning the making available on the market and use of biocidal products”. In: *Official Journal of the European Union* L 161 (2012-06-27), pp. 1–123. (accessed: 05.27.2019).
- [11] R. Dubey, T.C. Shami, and K.U. Bhasker Rao. “Microencapsulation Technology and Applications”. In: *Defence Science Journal* 59.1 (2009), pp. 82–95.

- URL: <http://citeseerx.ist.psu.edu/viewdoc/download?doi=10.1.1.849.9194rep=rep1type=pdf>. (accessed: 02.21.2019).
- [12] Jian-Zhong Ma et al. “Research advances in polymer emulsion based on “core–shell” structure particle design”. In: *Advances in Colloid and Interface Science* 197–198 (2013), pp. 118–131. DOI: 10.1016/j.cis.2013.04.006. (accessed: 05.23.2019).
- [13] Myer Kutz. *68.5.5 Anisotropy and Polarization*. John Wiley Sons, 2016. ISBN: 978-1-118-64724-0. URL: <https://app.knovel.com/hotlink/khtml/id:kt011BQCD3/handbook-measurement/anisotropy-polarization>. (accessed: 05.29.2019).
- [14] Hugo Valdés et al. “Experimental and Theoretical Approaches to the Influence of the Addition of Pyrene to a Series of Pd and Ni NHC-Based Complexes: Catalytic Consequences”. In: *Chemistry - A European Journal* 21.4 (2014), pp. 1578–1588. DOI: 10.1002/chem.201404618. URL: <https://onlinelibrary.wiley.com/doi/full/10.1002/chem.201404618>. (accessed: 04.24.2019).
- [15] Teresa M. Figueira-Duarte and Klaus Müllen. “Pyrene-Based Materials for Organic Electronics”. In: *Chemical Reviews* 111.11 (2011), pp. 7260–7314. DOI: 10.1021/cr100428a. URL: <https://pubs.acs.org/doi/pdf/10.1021/cr100428a>. (accessed: 04.24.2019).
- [16] *Pyrene*. URL: <https://pubchem.ncbi.nlm.nih.gov/compound/pyrene#section=Solubility>. (accessed: 05.28.2019).
- [17] Huai Nyin Yow and Alexander F. Routh. “Formation of liquid core–polymer shell microcapsules”. In: *Soft Matter* 2.11 (Aug. 2006), pp. 940–949. DOI: 10.1039/b606965g. (accessed: 02.19.2019).
- [18] Andrew Loxley and Brian Vincent. “Preparation of Poly(methylmethacrylate) Microcapsules with Liquid Cores”. In: *Journal of Colloid and Interface Science* 208.1 (1998), pp. 49–62. DOI: 10.1006/jcis.1998.5698.
- [19] Hirenkumar K. Makadia and Steven J. Siegel. “Poly Lactic-co-Glycolic Acid (PLGA) as Biodegradable Controlled Drug Delivery Carrier”. In: *Polymers* 3.3 (2011), pp. 1377–1397. DOI: 10.3390/polym3031377. (accessed: 02.14.2019).
- [20] Rajeev A Jain. “The manufacturing techniques of various drug loaded biodegradable poly(lactide-co-glycolide) (PLGA) devices”. In: *Biomaterials* 21.23 (2000), pp. 2475–2490. DOI: 10.1016/s0142-9612(00)00115-0. (accessed: 02.14.2019).
- [21] Sergio Freitas, Hans P. Merkle, and Bruno Gander. “Microencapsulation by solvent extraction/evaporation: reviewing the state of the art of microsphere preparation process technology”. In: *Journal of Controlled Release* 102.2 (2005), pp. 313–332. DOI: 10.1016/j.jconrel.2004.10.015.
- [22] Vitthal S. Kulkarni. *8.4.1 PLGA*. 2010. URL: <https://app.knovel.com/hotlink/khtml/id:kt00C5W014/handbook-non-invasive/plga>. (accessed: 05.13.2019).
- [23] Gustav Eriksson. “Microencapsulation of actives for the healthcare of tomorrow”. MA thesis. Sweden: Chalmers University of Technology, 2018.
- [24] S.m. Mirabedini, I. Dutil, and R.r. Farnood. “Preparation and characterization of ethyl cellulose-based core–shell microcapsules containing plant oils”. In:

- Colloids and Surfaces A: Physicochemical and Engineering Aspects* 394 (2012), pp. 74–84. DOI: 10.1016/j.colsurfa.2011.11.028. (accessed: 05.14.2019).
- [25] Deepak Bhatnagar and Fatima Hussain. “Omega-3 fatty acid ethyl esters (Omacor®) for the treatment of hypertriglyceridemia”. In: *Future Lipidology* 2.3 (2007), pp. 263–270. DOI: 10.2217/17460875.2.3.263. (accessed: 05.14.2019).
- [26] Sun Young Park et al. “Ethyl linoleate from garlic attenuates lipopolysaccharide-induced pro-inflammatory cytokine production by inducing heme oxygenase-1 in RAW264.7 cells”. In: *International Immunopharmacology* 19.2 (2014), pp. 253–261. DOI: 10.1016/j.intimp.2014.01.017. (accessed: 05.14.2019).
- [27] William Stillwell and Stephen R. Wassall. “Docosahexaenoic acid: membrane properties of a unique fatty acid”. In: *Chemistry and Physics of Lipids* 126.1 (2003), pp. 1–27. DOI: 10.1016/s0009-3084(03)00101-4. (accessed: 02.20.2019).
- [28] L. C. Stene et al. “Use of cod liver oil during pregnancy associated with lower risk of Type I diabetes in the offspring”. In: *Diabetologia* 43.9 (2000), pp. 1093–1098. DOI: 10.1007/s001250051499. (accessed: 05.28.2019).
- [29] Lloyd A. Horrocks and Young K. Yeo. “Health Benefits Of Docosahexaenoic Acid (Dha)”. In: *Pharmacological Research* 40.3 (1999), pp. 211–225. DOI: 10.1006/phrs.1999.0495. (accessed: 02.20.2019).
- [30] D.J. Undersander et al. URL: <https://hort.purdue.edu/newcrop/afcm/jojoba.html>. (accessed: 04.18.2019).
- [31] Jaime Wisniak. “Jojoba oil and derivatives”. In: *Progress in the Chemistry of Fats and other Lipids* 15.3 (1977), pp. 167–218. DOI: 10.1016/0079-6832(77)90001-5. (accessed: 04.18.2019).
- [32] Mark F McCarty. “Tributyryn May Have Practical Potential for Improving Cognition in Early Alzheimer’s Disease Via Inhibition of HDAC2”. In: (). URL: [http://catalyticlongevity.org/prepub\\_archive/Tributyryn-AD.pdf](http://catalyticlongevity.org/prepub_archive/Tributyryn-AD.pdf). (accessed: 04.24.2019).
- [33] Barbara A Conley et al. “Phase I study of the orally administered butyrate prodrug, tributyrin, in patients with solid tumors.” In: *Clinical Cancer Research* 4.3 (1998), pp. 629–634. (accessed: 04.24.2019).
- [34] Filip Van Immerseel et al. *COMPOSITION INHIBITING GRAM-NEGATIVE PATHOGENS IN GALLOANSERANS*. June 2016. (accessed: 04.24.2019).
- [35] Michael Ash and Irene Ash. *Trioctanoin*. 2003; 2013. URL: <https://app.knovel.com/hotlink/khtml/id:kt00BHXN72/handbook-solvents-2nd/trioctanoin>. (accessed: 05.14.2019).
- [36] Dimitrios Boskou. AOCs Press, 2006, pp. 41–72. ISBN: 978-1-893997-88-2. URL: <https://app.knovel.com/hotlink/toc/id:kp00CTE004/olive-oil-chemistry-technology/olive-oil-chemistry-technology>.
- [37] Frank Gunstone. *Vegetable Oils in Food Technology: Composition, Properties and Uses*. 2nd ed. Wiley, 2011.
- [38] T. Deutschle et al. “In vitro genotoxicity and cytotoxicity of benzalkonium chloride”. In: *Toxicology in Vitro* 20.8 (2006), pp. 1472–1477. DOI: 10.1016/j.tiv.2006.07.006.

- [39] Maximilian Lackner and Josef Peter Guggenbichler. “Antimicrobial Surfaces”. In: *Ullmanns Encyclopedia of Industrial Chemistry* (2013), pp. 1–13. DOI: 10.1002/14356007.q03\_q01.
- [40] Virinchipuram S. Sreevidya et al. “Benzalkonium chloride, benzethonium chloride, and chloroxylenol - Three replacement antimicrobials are more toxic than triclosan and triclocarban in two model organisms”. In: *Environmental Pollution* 235 (2018), pp. 814–824. DOI: 10.1016/j.envpol.2017.12.108.
- [41] Philippe Daull, Frédéric Lallemand, and Jean-Sébastien Garrigue. “Benefits of cetalkonium chloride cationic oil-in-water nanoemulsions for topical ophthalmic drug delivery”. In: *Journal of Pharmacy and Pharmacology* 66.4 (2013), pp. 531–541. DOI: 10.1111/jphp.12075. (accessed: 05.15.2019).
- [42] T. Koburger et al. “Standardized comparison of antiseptic efficacy of triclosan, PVP-iodine, octenidine dihydrochloride, polyhexanide and chlorhexidine digluconate”. In: *Journal of Antimicrobial Chemotherapy* 65.8 (2010), pp. 1712–1719. DOI: 10.1093/jac/dkq212. (accessed: 02.15.2019).
- [43] Grit Baier et al. “Enzymatic degradation of poly(l-lactide) nanoparticles followed by the release of octenidine and their bactericidal effects”. In: *Nanomedicine: Nanotechnology, Biology and Medicine* 10.1 (2014), pp. 131–139. DOI: 10.1016/j.nano.2013.07.002. (accessed: 02.18.2019).
- [44] *Octenidine*. URL: <https://www.drugbank.ca/drugs/DB12624>. (accessed: 05.29.2019).
- [45] Krister Holmberg, Bengt Kronberg, and Björn Lindman. *Surface Chemistry of Surfactants and Polymers*. Wiley, 2014. ISBN: 9781119961246.
- [46] Thaís M.c. Maria et al. “The effect of the degree of hydrolysis of the PVA and the plasticizer concentration on the color, opacity, and thermal and mechanical properties of films based on PVA and gelatin blends”. In: *Journal of Food Engineering* 87.2 (2008), pp. 191–199. DOI: 10.1016/j.jfoodeng.2007.11.026. (accessed: 05.29.2019).
- [47] Garba O. Yahya, S.k. Asrof Ali, and Esam Z. Hamad. “Surface and interfacial activities of hydrophobically modified poly(vinyl alcohol) (PVA)”. In: *Polymer* 37.7 (1996), pp. 1183–1188. DOI: 10.1016/0032-3861(96)80845-7. (accessed: 05.29.2019).
- [48] *Polyvinyl alcohol*. URL: <https://pubchem.ncbi.nlm.nih.gov/compound/Ethenol>. (accessed: 03.03.2019).
- [49] L. Fallon and PhD Fleming Jr. “Microscopy.” In: *Magill’s Medical Guide (Online Edition)* (2018). URL: <http://proxy.lib.chalmers.se/login?url=http://search.ebscohost.com/login.aspx?direct=true&db=ers&AN=87690582&site=eds-live&scope=site>. (accessed: 05.09.2019).
- [50] Alberto Fernandez-Nieves and Antonio Manuel Puertas. *10.3 Bright Field and Dark Field Microscopy*. 2016. URL: <https://app.knovel.com/hotlink/khtml/id:kt011HFI9M/fluids-colloids-soft/bright-field-dark-field>. (accessed: 05.09.2019).
- [51] *Role of Microscopy*. Feb. 2015. URL: <https://clinicalgate.com/role-of-microscopy/>. (accessed: 05.09.2019).

- 
- [52] Thomas E. Creighton. *8.2.2 Fluorescence Microscopy*. 2010. URL: <https://app.knovel.com/hotlink/khtml/id:kt0091X3S1/physical-chemical-basis/fluorescence-microscopy>.
- [53] Erik Oberg et al. *45.9.4 Drop Size Measurement*. 2016. URL: <https://app.knovel.com/hotlink/khtml/id:kt010ZUGX1/machinerys-handbook-30th/drop-size-measurement>. (accessed: 05.09.2019).
- [54] Colin McPhee, Jules Reed, and Izaskun Zubizarreta. *6.2.1.2 The Pendant Drop Method*. 2015. URL: <https://app.knovel.com/hotlink/khtml/id:kt010WAZ52/core-analysis-best-practice/pendant-drop-method>. (accessed: 05.09.2019).
- [55] Donald L. Pavia et al. *Introduction to spectroscopy*. 5th ed. Cengage Learning, 2015.
- [56] Petrus Jakobsen. “Antiseptic microspheres embedded in nonwoven fiber materials”. MA thesis. Sweden: Chalmers University of Technology, 2019.
- [57] Viktor Eriksson. “Core-shell particles based on biopolymers and bioactive fatty acids: encapsulation, characterization and release”. MA thesis. Sweden: Chalmers University of Technology, 2019.



# A

## Microscopy images from the benzalkonium chloride encapsulation

In following chapter, images attained both by bright field microscopy and fluorescence microscopy from the benzalkonium chloride encapsulation are presented.

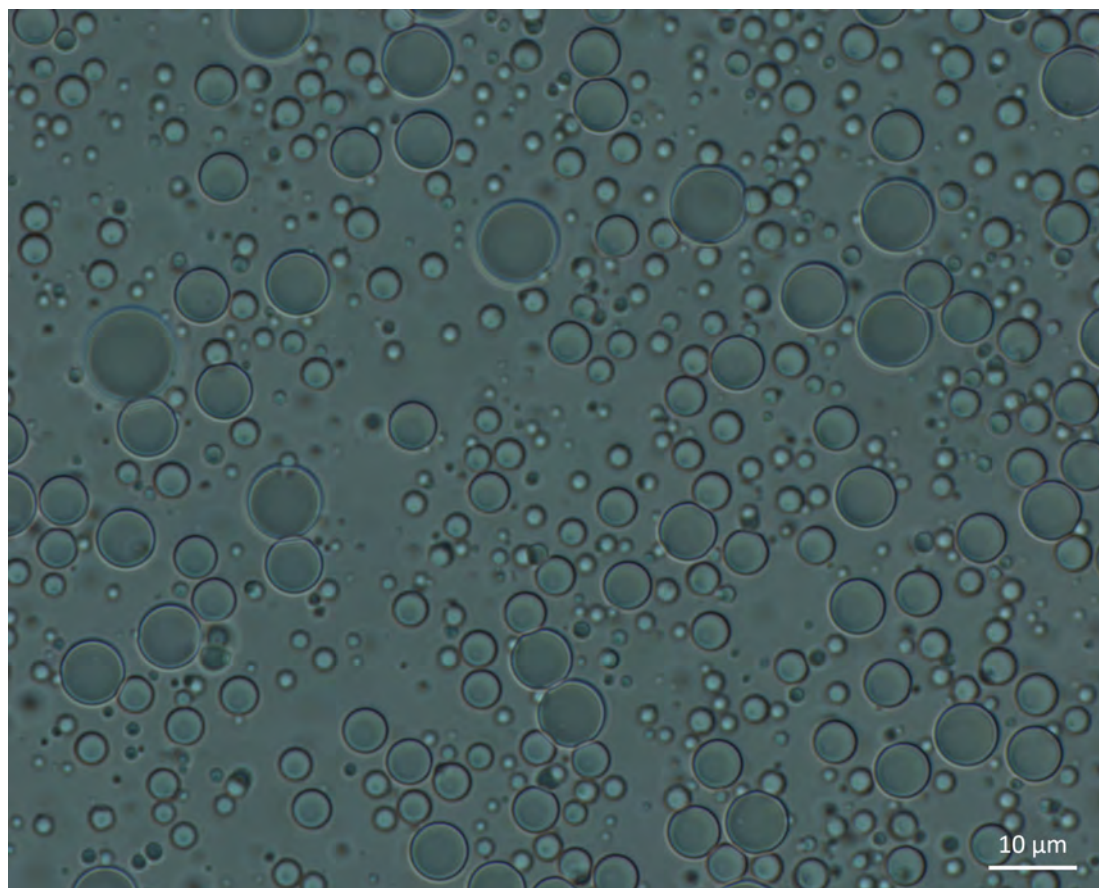
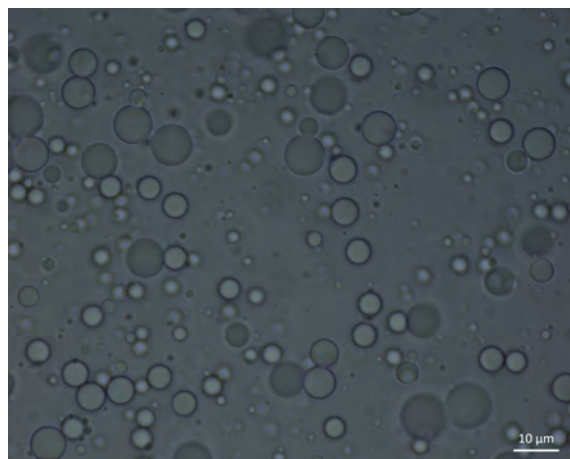
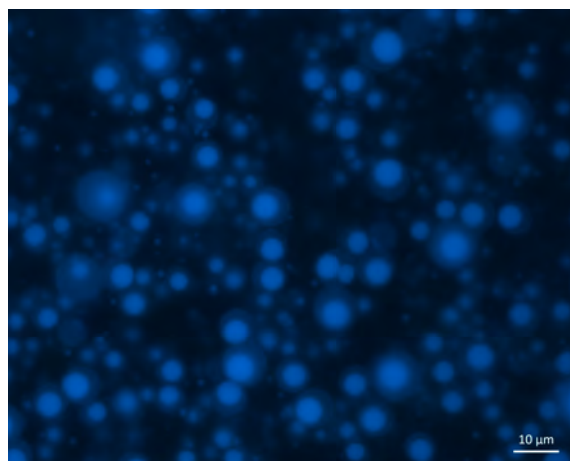


**Figure A.1:** A representative image of ethyl linoleate/benzylkonium chloride microcapsules, obtained from bright field microscopy (100x magnification).



(a)



(b)

**Figure A.2:** Two representative images of olive oil/benzalkonium chloride microcapsules, obtained from (a) bright field and (b) fluorescence microscopy (both 100x magnification).

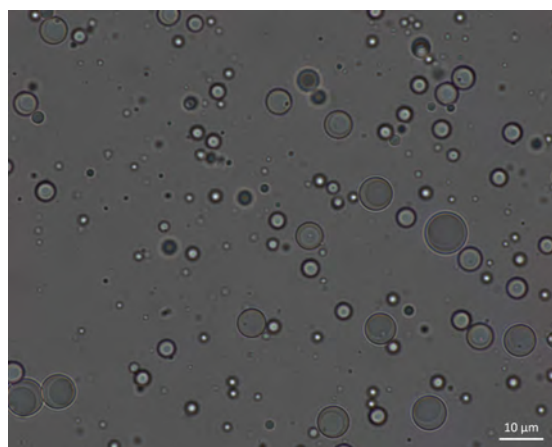
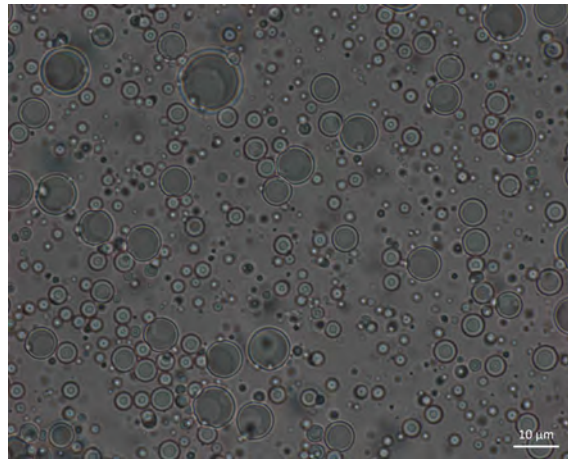
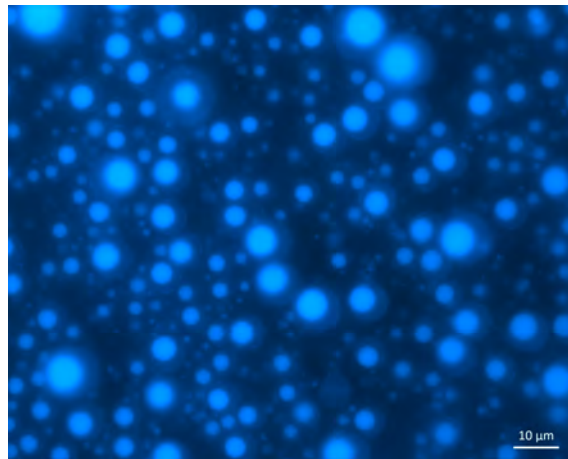


**Figure A.5:** A representative image of docosahexanoic acid methyl ester/benzylkonium chloride microcapsules, obtained from bright field microscopy (100x magnification).



(a)



(b)

**Figure A.3:** Two representative images of glyceryl trioctanoate/benzalkonium chloride microcapsules, obtained from (a) bright field and (b) fluorescence microscopy (both 100x magnification).

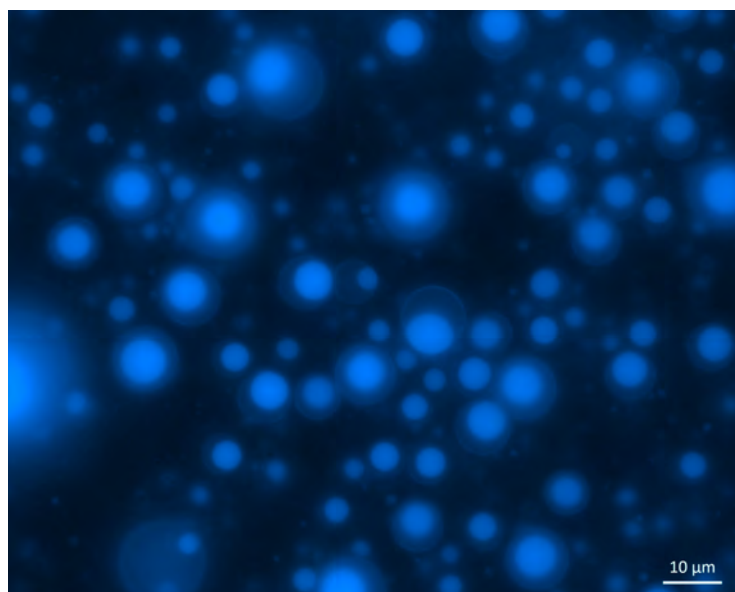
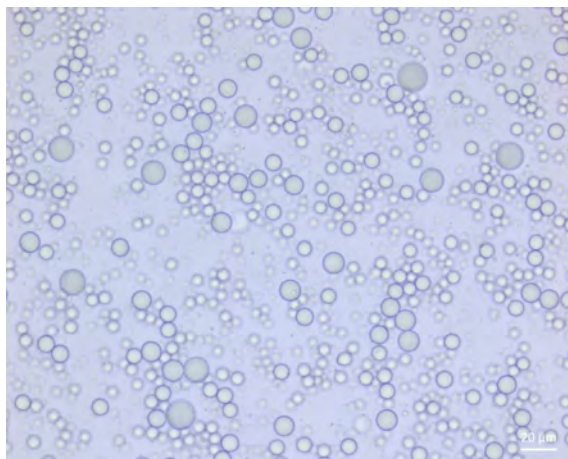
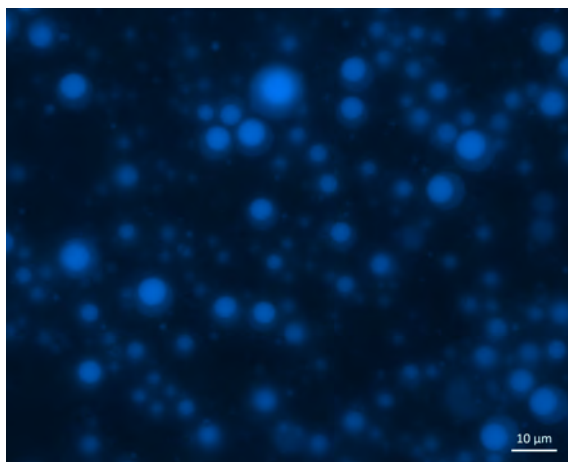


**Figure A.6:** A representative image of jojoba oil/benzylkonium chloride microcapsules, obtained from fluorescence microscopy (100x magnification).



(a)



(b)

**Figure A.4:** Two representative images of sunflower oil/benzalkonium chloride microcapsules, obtained from (a) bright field (40x magnification) and (b) fluorescence microscopy (100x magnification).

# B

## Yield of deprotonated octenidine

The percent yield is calculated according to following equation (equation B.1):

$$\text{Percent Yield} = \frac{\text{actual yield}}{\text{theoretical yield}} \times 100 \quad (\text{B.1})$$

The weight of the final product was 0.559 g. Hence, the *actual yield* was 0.559 g. The weight of the octenidine dihydrochloride used for the conversion was 1.9 g. Knowing that the molar mass of deprotonated octenidine (DPO) is 587.38 g/mol and 623.84 g/mol for octenidine dihydrochloride (OCT), the *theoretical yield* could be calculated:

$$n(\text{OCT}) = \frac{m(\text{OCT})}{M(\text{OCT})} = \frac{1.9 \text{ g}}{623.84 \text{ g/mol}} = 0.00305 \text{ mol} \quad (\text{B.2})$$

Since  $n(\text{OCT})=n(\text{DPO}) \implies$

$$m(\text{DPO}) = n(\text{DPO}) * M(\text{DPO}) = 0.00305 \text{ mol} * 587.38 \text{ g/mol} = 1.789 \text{ g} \quad (\text{B.3})$$

Hence, the theoretical yield is 1.789 g. Consequently, the yield of deprotonated octenidine dihydrochloride:

$$\text{Percent Yield} = \frac{0.559 \text{ g}}{1.789 \text{ g}} \times 100 = \mathbf{31.247 \%} \quad (\text{B.4})$$



# C

## Interfacial tension measurements for deprotonated octenidine and octenidine dihydrochloride

In Table C.1, the interfacial tensions obtained from deprotonated octenidine and octenidine dihydrochloride at different weight percents dissolved in dichloromethane are presented. The aqueous phase contained 5 wt% PVA.

**Table C.1:** Interfacial tension of deprotonated octenidine (DPO) and octenidine dihydrochloride (OCT) as a function of weight percent. The compounds were dissolved in dichloromethane and immersed in 5 wt% PVA-water-solution.

Weight percent	DPO (mN/m)	OCT (mN/m)
0.025	7.736	6.997
0.25	5.735	5.865
2.5	3.730	3.661
3.3	3.470	3.450
4.2	3.300	3.110
5	3,145	2.966
7.5	2.605	2.566
10	2.431	2.148
12.5	2.274	2.116
15	1.992	1.901